Journal of Materials Science

Volume No. 12

Issue No. 1

January - April 2024

ENRICHED PUBLICATIONS PVT. LTD

S-9, IInd FLOOR, MLU POCKET,
MANISH ABHINAV PLAZA-II, ABOVE FEDERAL BANK,
PLOT NO-5, SECTOR-5, DWARKA, NEW DELHI, INDIA-110075,
PHONE: - + (91)-(11)-47026006

Journal of Materials Science

Aims and Scope

The Journal of Materials Science is now firmly established as the leading source of primary communication for scientists investigating the structure and properties of all engineering materials. The Journal of Materials Science publishes reviews, full-length papers, and short communications recording original research results on, or techniques for studying the relationship between structure, properties, and uses of materials. The subjects are seen from international and interdisciplinary perspectives covering areas including metals, ceramics, glasses, polymers, electrical materials, composite materials, fibers, nanostructured materials, nanocomposites, and biological and biomedical materials.

Journal of Materials Science

Journal of Materials Science

(Volume No. 12, Issue No. 1, Jan - Apr 2024)

Contents

A Review on Thermoelectric Generator Used in Automotive Waste Heat Recovery

Vikrant Mishra[1], Amit Pal[2]
[1]P.G. Student, Mechanical Department, Delhi Technological University, Bawana Road Delhi-110042,
E-mail- mishra92vikrant@gmail.com,
[2]Associate Professor, Mechanical Department, Delhi Technological University, Bawana Road Delhi-110042
E-mail- amitpal@dce.ac.in

A B S T R A C T

The increasing demand for electric power in passenger vehicles has motivated several research and advancement since the last two decades. This demand has been revaluated by the unrelenting, rapidly growing reliance on electronics in modern vehicles. Thermoelectric Generators can generate electrical energy by utilizing waste heat of automobile exhaust gases on the basis of Seebeck Effect. This paper presents the review of previous work done related to thermoelectric conversion from automobile exhaust gases. Most of the previous researches are related to design consideration of heat exchangers used in complete unit of thermoelectric generator, but there is a few literature about power loss during module mismatching when two or more thermoelectric generators are electrically connected. This paper also presents the concept of module mismatch in the operation of thermoelectric generator. If power loss due to module mismatching could be minimized, the thermal of electrical conversion efficiency of the system will increase significantly.

Keywords- Thermoelectric Generator; Seebeck effect; Heat exchanger; Module Mismatch.

1. INTRODUCTION

In recent years, Energy crisis has become a major challenge due to quickly increasing demands and consumption of Energy. The scientific and public awareness on environmental and energy issue has brought in key interest to the advancement in technologies and research particularly in highly efficient internal combustion engines. Generally, there are two basic methods to improve efficiency of internal combustion engine. First method is optimization of combustion process and second is to recover waste heat of the engine exhaust gases. In a typical IC engine driven automobile, Vehicle mobility and accessories utilize only about 25% of the supplied fuel energy. During the combustion process in an automobile engine, 40% of the energy is lost through exhaust gases and about 30% is reflected in the form of the heat carried away by the engine coolant liquid [1].So, an effort should be made to capture a significant portion of the available heat energy of exhaust gases. It can not only help in reducing engine loads and alternator size but also decrease pollutant emissions and fuel consumption [2]. There are many waste heat recovery (WHR) technologies such as Rankine bottoming cycle technique, Six-

stroke internal combustion engine cycle technique, Turbocharger and Thermoelectric energy conversion technique [3]. But thermoelectric power generation technique directly convert thermal energy into electrical energy. Moreover, Thermoelectric Generator (TEG) has no moving parts and it is compact, quiet, highly reliable and environmentally friendly.

In 1821, Thomas Johann Seebeck discovered the phenomenon of thermoelectricity. When a temperature gradient is established between the hot and cold junctions of two dissimilar materials (metals or semiconductors), a voltage is generated, i.e., Seebeck Voltage. Based on this Seebeck effect, thermoelectric devices can act as electrical power generators [4]. The major drawback of thermoelectric generator is their relatively low conversion efficiency (typically 5-10%). Therefore, TEGs have mostly been used in specialized electrical equipment in aerospace and military applications [5]. With technological advancement in the last two decades, The TEG has shown ever increasing potential for application that can be widely used in power generation from automobile exhaust waste heat, industrial waste heat, solar energy and other natural thermal energies.

The total energy consumption in India, as per Global Energy Statistical yearbook 2015, is 872 Mtoe. The transportation sector consumes approximately 30% (261.6 Mtoe) of the total energy consumption [6]. So there is a great scope for thermoelectric power generator in automotive applications, which can reduce fuel consumption.

2. SEEBECK EFFECT

Seebeck effect is the direct conversion of temperature gradient into electricity. Basically, the materials used to generate Seebeck effect are two different metals or semiconductors. The output is a measure of the magnitude of an induced thermoelectric voltage in response to a temperature difference across that material. In Figure 1, the materials used in the two legs are N and P-type semiconductors. The open circuit voltage V_{oc} generated by this TE couple is then governed by the equation

$$V_{oc} = \int_{T_c}^{T_h} (S_n(T) - S_p(T))\mathrm{d}T \quad (1)$$

(1):

Where S_n and S_p are Seebeck Coefficients for N-type and P-type semiconductors respectively.

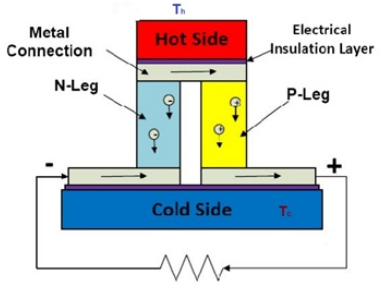

Figure 1.Basic illustration of Seebeck Effect

If the Seebeck coefficients are approximately constant for the measured temperature range in the TE legs (which is often true), Equation (1) can be simplified as [7]:

$$V_{oc} = (S_n - S_p) \cdot (T_h - T_c) \quad (2)$$

If the temperature difference ΔT between the two ends of a material is small, then the Seebeck coefficient of this material is approximately defined as [7]:

$$S = \frac{\Delta V}{\Delta T} \quad (3)$$

where ΔV is the voltage seen at the terminals.

3. THERMOELECTRIC MATERIALS

Attempts are being made to improve the performance of thermoelectric material by improving the figure-of-merit. Saniya LeBlanc [8] discussed about new thermoelectric materials and material performance. The classification of TE materials is based on material structure and composition. Generally chalcogenide, skutterudite, clathrate, half-heusler, silicide and oxide are some types of TE materials.

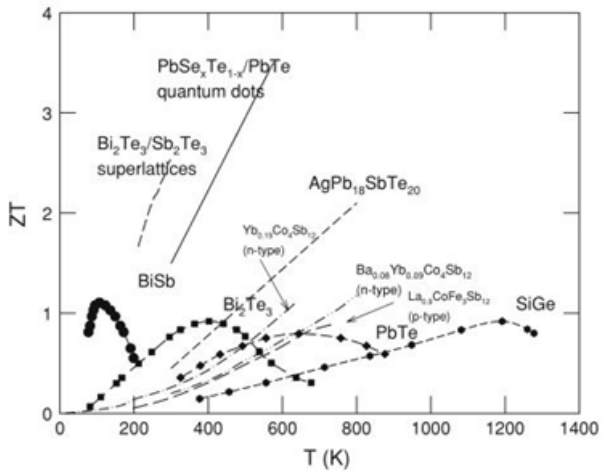

Figure 2. Figure of merit (ZT) versus Temperature curves. [9]

In these types, Chalcogenide materials are widely used in demonstrated thermoelectric application with bismuth telluride (Bi_2Te_3) and lead telluride (PbTe) being the most noticeable. Bismuth Telluride and its solid solution with antimony and selenium are commercially used for thermoelectric modules in case of low temperature. Whenever there are higher temperatures (500~600˚C), Lead Telluride is used for better thermoelectric properties. The properties of TE materials mainly depend on temperature which emphasize multiple challenges for application-specific materials selection.

4. ANALYSIS OF PREVIOUSLY DEVELOPED MODELS OF TEG

Wang et al. [10] presents a mathematical model of a Thermoelectric Generator (TEG) device using the exhaust gas of vehicles as heat source based on Fourier's law and Seebeck Effect. The model pretends the influence of various related factors on the output power and efficiency, such as vehicles exhaust mass flow rate, mass flow rate of different types of coolants, temperature of exhaust gas, temperature difference across TEG, convection heat transfer coefficient, height of P-N couple and the ratio of external electrical resistance to internal resistance of the circuit on the output power and efficiency of the TEG system. The results showed that the output power and efficiency increase significantly by varying the convection heat transfer coefficient of the high-temperature-side than that of low-temperature-side. The results also showed that the power output achieved a peak value for optimum height of P-N couple. Besides it the peak output power value decreases when the thermal conductivity of the PN couple is decreased, and increases when the Seebeck coefficient and electric conductivity of the material are increased. Additionally, a maximum value of power output and efficiency of TEG device appear when external electrical resistance is greater than internal resistance. This is not usual as common circuit and with the augmentation of dimension-less figure of merit (ZT), the maximum value of output moves toward the direction of an increasing ratio of external resistance to internal resistance.

Zhang et al. [11] designed, employed and compared the parallel-connected thermoelectric power generator system. The advantage of this system is that it provide dual DC bus and it has high overall system efficiency. The low efficiency in the pure battery discharging mode can be evaded with other switching circuit. So this parallel-connected system is a superior choice for automotive application excluding the series-connected system.

Martins et al. [12] assessed the potential of the use of heat pipes (HP) as a means of transferring energy from the hot exhaust gases to the TEG modules at a well-suited temperature level while diminishing the loss of efficiency due to reducing temperature. In this work, Variable Conductance Heat Pipe (VCHP) was used and its arrangement has the benefit of inducing good temperature control. Various types of heat pumps were designed, manufactured, verified and improved with the purpose of enhancing the overall heat transfer process, enabling an optimal level of electric energy recovery using proper arrangement of TEG modules. The results indicate that the use of VCHPs in conjunction with thermoelectric generators is a convincing technique for recovering waste heat energy from the automobile exhaust gases.

Tongcaiet al. [13] proposed a new type of open-cell metal foam-filled plate heat exchanger based thermoelectric generator (TEG) system to utilize low grade waste heat. In this system thermoelectric

generation works as a parasitic mode which is attached to heat exchanging process. The major portion of waste heat is captured by the process of heating water and an amount of this waste heat flux is converted by means of TEG into electricity as by product. Performance of TEG is much dependent of the temperature difference. The open circuit voltage of One TE couple increased approximately linearly from 0 to 5.5 mV with the variation of temperature difference from 0 to 13.8˚C. When load resistance becomes equal to internal resistance, maximum power output of one TE couple was obtained. The feasibility of increasing the number of TE couples was also demonstrated which helps in enlarging the electricity generation capacity. The maximum open circuit voltage increases up to 108.1 mV from 5.5 mV, when the number of TE couples was varied from 1 to 16.

Orr et al. [14] presented a combination of two promising technologies to recover waste heat of automobile exhaust. The useful two technologies for this purpose were thermoelectric cells (TECs) and heat pipes. In this work a bench type model was demonstrated which produced power by Thermo electric cells using heat pipes. The heat to electrical conversion efficiency of whole system was found 1.43% and the predicted efficiency was 2.31%. The difference between predicted and actual efficiency was due to the cells not operating at their optimum voltage.

5. DESIGN CONSIDERATIONS OF AUTOMOTIVE TEG SYSTEM

For an efficient automotive thermoelectric generator system, the designs of the complete device and its components are considerably significant. Design of Heat Exchangers, Optimization of Fin distribution and Thermal performance of heat exchangers are very important parameters which should be optimized while designing the complete assembly of TEG system. The overall conversion efficiency also increases when design heat exchanger is optimized. In the last decade, more researchers have worked in this area which gave better result in the sense of making automotive TEG system commercial in automobile industries.

Deng et al. [15] discussed the thermal performance of the heat exchanger in automobile exhaust based thermoelectric generator. Various internal structures of heat structures were applied with different TE materials. This thermal optimization is done by the computational fluid dynamics (CFD) simulation and then by infrared image capture experiment. For CFD simulation two 3-dimensional models of hexagonal-prism-shaped and plate-shaped heat exchangers were designed and taken into consideration. CFD simulation results show that the interface temperature for hexagonal prism-shaped heat exchanger is just around 120˚C which is far less than the required temperature of hot side of automotive TEG system. But in case of plate-shape heat exchanger with several baffle plates, the

interface temperature is around or sometimes more than 240˚C. Additionally, the volume of hexagonal prism-shaped heat exchanger is very large compared to plate shaped heat exchanger which is not advantageous due to greater heat loss. So all results depicted that plate shaped heat exchanger are more suitable for waste heat recovery using TEG device.

Liu et al. [16] simulated the design of heat exchanger with different internal structure. In the first case, no internal fins were used which caused sudden expansion of exhaust gas flowing through the pipe. Uneven thermal distribution occurred inside the heat exchanger and the outside temperature found (144˚C) was less and heat exchanger could not meet the requirement. So after this, two 3-dimensional models of heat exchangers with fishbone-shaped and chaos-shaped internal structures were designed. Simulation results showed that heat exchanger with chaos-shaped internal structure have higher outlet temperature (220˚C on average) than in case of fishbone-shaped (190˚C). Thus, Chaos-shaped heat exchanger design is more ideally suitable in TEG application. Additionally, the thickness of the heat exchanger is also responsible for thermal performance. Heat exchanger of chaos-shaped internal structure with different thicknesses of 3 mm, 5 mm and 8 mm respectively were used for simulation comparison. The results shows that in case of 3 mm thickness heat exchanger the outlet temperature is approximately 180˚C which is lesser than expected hot side temperature in automotive TEG application. So heat exchanger with 5 mm and 8 mm thicknesses were used and there was little difference in the interface temperatures. So the lighter size of TEG (5 mm thickness) is better because of reduction in weight.

DeokIn et al. [17] presented various types of heat sinks used in automotive exhaust based thermoelectric generator. The types used were rectangular pillar-shaped heat sink, forward facing triangular pillar heat sink and backward facing triangular pillar heat sink. The generated peak voltage measured for rectangular heat sink was approximately 2.7 V which was higher than generated 2.5 V and 2.4 V in forward facing and reverse facing triangular heat sink respectively.

Ramade et al. [18] presented thermal optimization technique of thermoelectric generator system with different kinds of heat sink. The observed efficiency was not quite in case of single stacked type cold side heat sink, so thermal optimization of system is done to improve efficiency. Double stacked type heat sink was used which gave better temperature difference across TEG. Thermal insulation was applied on the uncovered area to neglect heat loss and counter flow type heat exchanger was arranged which increased the effective heat transfer. Results were obtained with Bismuth-Telluride thermoelectric material at hot side temperature of 250˚C. Result show that efficiency of TEG device and power developed increases with increase in speed of engine. The efficiency of TEG device was 5.0708% and power generated was 15.12 W at engine speed of 3970 rpm.

Su et al. [19] presented experimental study on thermal optimization of the heat exchanger in an automobile exhaust-based thermoelectric generator. In order to achieve temperature uniformity and higher interface temperature, three-dimensional models of different types of heat exchangers were developed and then compared with the help of CFD simulation. These types of internal structure of heat exchangers are fishbone-shaped, accordion-shaped and scatter-shaped. The CFD simulation result indicates that the accordion-shaped internal structure of heat exchanger provide a better uniform temperature distribution and it has also higher interface temperature than the other two internal structures.

Yiping et al. [20] discussed about optimization of fin distribution to maximize the electrical power generated. A CFD model of heat exchanger was constructed to describe the effect of various fin distributions on the temperature uniformity. Four Factors: length of fins, spacing between the fins, angle of fins and thickness of the fins, were considered for the optimization of fin distribution. Optimization of these four factors improved the temperature uniformity without too great pressure loss.

Bai et al. [21] presented CFD analysis of heat exchangers used in automotive TEG with six different designs. This CFD analysis was done to compare the pressure drop and heat transfer for all six different structures of heat exchanger. The descending order of heat transfer as follows: serial plate structure, separate plate with holes, parallel plate structure, pipe structure, inclined plate structure and empty cavity. The descending order of pressure drop is same for all structures except the pipe structure which has the 2^{nd} highest pressure drop.

6. MODULE MISMATCH

There is a little literature available on the issue of module mismatch in thermoelectric generators. When two or more thermoelectric modules are connected, the combined power is less than the sum of individual power outputs of the modules. This phenomenon is known as module mismatch.

Nagayoshi et al. [22] introduced mismatching in their work and developed a Maximum Power Point Tracking (MPPT) system. The MPPT power conditioner consists of internal power supply, a Buck-Boost converter and micro controller. MPPT system can increase conversion efficiency but particularly in case of transients system. When thermoelectric generators are in steady state, MPPT system are not so useful but it still has the ability to cause the modules to operate at their peak power. In this work, no analytical analysis was presented to find the source of mismatch.

Module mismatching in case of thermoelectric modules is quite similar to the mismatching in photovoltaic arrays. So the mismatch losses concepts in PV arrays should be considered in the development of the thermoelectric module mismatch predictive equations. Chouder and Silvestre [22] presented experimental and modeling results on mismatch effects in PV modules. In this study, power losses were observed around 10% associated with mismatch between PV modules forming the PV array. Picault et al. [23] developed several connection schemes for each of the PV modules and analyzed the mismatch losses for each of the connection schemes. Because of the similarities between photo voltaics and thermo electrics, parallels can be drawn with regards to performance. There is need of further exploration to conclude the significance of the module mismatch effect for thermoelectric modules.

7. CONCLUSION

This paper presents a brief review of automobile exhaust based thermoelectric generator which use exhaust gas of vehicle as a heat source and convert this heat energy into electrical energy on the basis of Seebeck effect. Most of the previous researches are focused on the making efficient TEG system. So some other technologies suchas variable conductance heat pipes and open cell metal foam-filled heat exchanger, are used along with the use of TEG. The combined system of heat pipes or heat exchanger with TEG made the complete waste heat recovery unit efficient. This paper also presented the various design considerations of heat exchanger. It can be depicted that for higher conversion efficiency the proper internal structure of heat exchanger is needed. In the end, the concept of mismatch is introduced in case when two or more modules are electrically linked. Further research should be focused on increasing conversion efficiency of complete waste heat recovery unit and modules should operate at optimum parameters.

8. REFERENCES

[1] P. Aranguren, D. Astrain, A. Rodríguez, and A. Martínez, Experimental investigation of the applicability of a thermoelectric generator to recover waste heat from a combustion chamber, Applied Energy, 2015 Vol. 152, pp. 121-130. http://www.sciencedirect.com/science/article/pii/S0306261915005401

*[2] F. Stabler, Automotive Thermoelectric Generator Design Issues, Thermoelectric Applications Workshop, March 24-27, 2002,pp.1-24.*https://www1.eere.energy.gov/vehiclesandfuels/pdfs/thermoelectrics_app_2009/wednesday/stabler.pdf

[3] R. Saidur, M. Rezaei , W.K. Muzammil, M.H. Hassan, S. Paria, M. Hasanuzzaman, Technologies to recover exhaust heat from internal combustion engines, Renewable and Sustainable Energy Reviews 2012, Vol. 16, pp.5649–5659. http://hir.um.edu.my/images/hir/doc/publication/Dr.Saidur_Techn.pdf

[4] Basel I. Ismail and Wael H. Ahmed, Thermoelectric Power Generation Using Waste-Heat Energy as an Alternative Green Technology, Recent Patents on Electrical Engineering 2009, Vol. 2 No. 1, pp. 27-39. http://benthamscience.com/journals/recent-advances-in-electrical-and-electronic-engineering/volume/2/issue/1/page/27/

[5] D. Crane, G. Jackson and D. Holloway, Towards optimization of automotive waste heat recovery using thermoelectrics, SAE Technical Paper 2001, pp. 10-21. http://papers.sae.org/2001-01-1021/https://yearbook.enerdata.net/
[6] accessed on April 20, 2016.http://www.efunda.com/designstandards/sensors/thermocouples/thmcple_theory.cfm?search_string=thermoelectric%20effect
[7] http://www.efunda.com/designstandards/sensors/thermocouples/thmcple_theory.cfm?search_string=thermoelectric%20effect accessed on April 20, 2016.
[8] Saniya LeBlanc, Thermoelectric generators: Linking material properties and systems engineering for waste heat recovery applications, Sustainable Materials and Technologies 2014, Vol.1-2, pp. 26–35. http://www.leblanclab.com/uploads/2/6/4/3/26439896/thermoelectric_generators_linking_material_properties_and_systems_engineering_for_waste_heat_recovery_applications leblanc.pdf
[9] Yang J. and Stabler F. R., Automotive Applications of Thermoelectric Materials, J. Elec. Materials 2009, Vol. 38, pp. 1245–1251. http://link.springer.com/article/10.1007/s11664-009-0680-z
[10] Yuchao Wang, Chuanshan Dai and Shixue Wang, Theoretical analysis of a thermoelectric generator using exhaust gas of vehicles as heat source, Applied Energy 2013, Vol. 112, pp. 1171–1180. http://econpapers.repec.org/article/eeeappene/v_3a112_3ay_3a2013_3ai_3ac_3ap_3a1171-1180.htm
[11] X. Zhang, K. T. Chau and C. C. Chan, Design and implementation of a thermoelectric-photovoltaic hybrid energy source for hybrid electric vehicles, World Electric Vehicle Journal, Vol. 3, Dec. 2009, pp. 1-11. http://www.evs24.org/wevajournal/php/download.php?f=vol3/WEVJ3-2130104.pdf
[12] Jorge Martins, Francisco P. Brito, L.M.Goncalves and Joaquim Antunes, Thermoelectric Exhaust Energy Recovery with Temperature Control through Heat Pipes, SAE 2011-01-0315, 2011.
http://www.evs24.org/wevajournal/php/download.php?f=vol3/WEVJ3-2130104.pdf
[13] Tongcai Wang, Weiling Luan, Wei Wang, Shan-Tung Tu, Waste heat recovery through plate heat exchanger based thermoelectric generator system, Applied Energy 2014, Vol. 136, pp. 860–865. http://www.sciencedirect.com/science/journal/03062619/136
[14] B. Orr, B. Singh, L. Tan, A. Akbarzadeh, Electricity generation from an exhaust heat recovery system utilizing thermoelectric cells and heat pipes, Applied Thermal Engineering 2014, Vol. 73, pp. 588-597. http://www.sciencedirect.com/science/journal/13594311/73/1
[15] Y. D. Deng, X. Liu, S. Chen and N. Q. Tong, Thermal Optimization of the Heat Exchanger in an Automotive Exhaust-Based Thermoelectric Generator; Journal of Electronic Materials 2013, Vol. 42, No. 7, DOI: 10.1007/s11664-012-2359-0. http://link.springer.com/article/10.1007%2Fs11664-012-2359-0
[16] X. Liu, Y.D. Deng, K. Zhang, M. Xu, Y. Xu, C.Q. Su, Experiments and simulations on heat exchangers in thermoelectric generator for automotive application, Applied Thermal Engineering 2014, Vol. 71, pp. 364-370. http://www.sciencedirect.com/science/journal/13594311/71/1
[17] Byungdeok In, Hyungik Kim, Jung wook Son and Ki hyung Lee The study of a thermoelectric generator with various thermal conditions of exhaust gas from a diesel engine,International Journal of Heat and Mass Transfer 2015, Vol. 86, pp. 667–680. http://www.sciencedirect.com/science/journal/00179310/86
[18]PrathameshRamade, PrathameshPatil, ManojShelar, Sameer Chaudhary, Prof. Shivaji Yadav, Prof. Santosh Trimbake, Automobile Exhaust Thermo-Electric Generator Design & Performance Analysis, International Journal of Emerging Technology and Advanced Engineering, May 2014, Vol. 4, Issue 5, pp. 1-10. http://www.ijetae.com/files/Volume4Issue5/IJETAE_0514_104.pdf
[19] C.Q. Su, W.S. Wang, X. Liu, Y.D. Deng, Simulation and experimental study on thermal optimization of the heat exchanger for automotive exhaust-based thermoelectric generators, Case Studies in Thermal Engineering 2014, Vol. 4, pp. 85–91. http://www.sciencedirect.com/science/article/pii/S2214157X14000197
[20] Yiping Wang, Cheng Wu, Zebo Tang, Xue Yang, Yadong Deng and Chuqi Su, Optimization of Fin Distribution to Improve the Temperature Uniformity of a Heat Exchanger in a Thermoelectric Generator; Journal of Eletronic Materials 2015, Vol. 44, No. 6, DOI: 10.1007/s11664-014-3527-1. http://link.springer.com/article/10.1007/s11664-014-3527-1
[21] Shengqiang Bai, Hongliang Lu, Ting Wu, Xianglin Yin, Xun Shi, Lidong Chen; Numerical and experimental analysis for exhaust heat exchangers in automobile thermoelectric generators, Case Studies in Thermal Engineering 2014, Vol. 4, pp. 99–112. http://www.sciencedirect.com/science/article/pii/S2214157X14000252
[22] H. Nagayoshi, T. Nakabayashi, H. Maiwa, and T. Kajikawa, Development of 100-W HighEfficiency MPPT Power Conditioner and Evaluation of TEG System with Battery Load,Journal of Electronic Materials, 2011 Vol. 40, no. 5, pp. 657-661.
[23] A. Chouder and S. Silvestre, Analysis model of mismatch power losses in PV systems,Journal of Solar Energy Engineering, 2009 Vol. 131, no. 2, pp. 024504-1 – 024504-5.
[24] D. Picault, B. Raison, S. Bacha, J. de la Casa, and J. Aguilera, Forecasting photovoltaicarray power production subjest to mismatch losses,Solar Energy, 2010 Vol. 84, no. 7, pp. 1301-1309.

Design & Development of a Fixture to Study Biaxial Behavior of Engineering Materials in Tension

Vijay Gautam[1‡], Rakesh Singla[2], Sunil Kumar[3]
Department of Mechanical Engineering, Assistant Professor, DTU New Delhi 110042,
[1‡]vijay.dce@gmail.com, [2]rakeshsingla19@gmail.com and [3]sunil007mae@gmail.com

A B S T R A C T

The focus of this paper is to emphasize the need of the biaxial test that have been with primary focus on sheet metal forming. Biaxial testing of metal is becoming dominant in sheet metal for establishing the mechanical properties of the sheet material. The primary reason for using the biaxial tensile test, as opposed to uniaxial test, is that metal in sheet form is highly anisotropic. The reason behind such a large variation in properties is the use of forming process in manufacturing of the sheets. The uniaxial tensile test only determines the properties in one direction and that data is not sufficient for multi-directional forming processes such as deep drawing. Due to multi-directional loading the component fails at loads much less than that determined by uniaxial test. This is the main reason to develop a fixture for biaxial testing. The device can also be used for uniaxial testing by removing some linkages. This paper includes the design and analysis of the biaxial tensile test fixture. A brief description of the rapid prototyping of the fixture is also presented.

Keywords- Uniaxial Tension Test; Biaxial Tension Test; Fixture; Anisotropy; Rapid Prototyping.

1. INTRODUCTION

There is a continuous effort in the automotive industries to improve the capabilities of forming simulations in order to minimize the production costs of car components. This effort requires improvements to the currently used continuum models, especially after the reports on unpredicted damage-driven failures of the new advanced high strength steels like Tranformation induced plasticity (TRIP) and dual-phase steels (DP)[1-2]. In the biaxial strain path, for example, it is observed for these metals that the experimentally obtained fracture limit curve approaches the forming limit curve[3-4]. This type of damage-influenced fracture sensitivity is not captured in the currently used models. Furthermore, it has long been known that the formability limits of sheet metals are heavily dependent on the exact strain path that they follow, as shown in fig. 1[5].

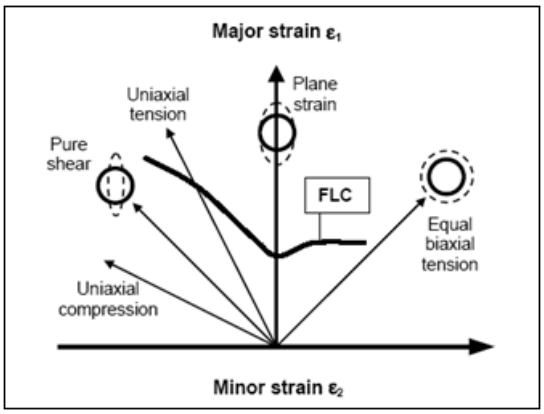

Fig. 1 Forming limit diagram [5]

Complex forming paths are frequently used in the industry to improve the formability of the sheets. However, most forming simulations used in the industry are not equipped with suitable tools to accurately predict the strain path dependency of the sheet to be formed. Improving the predictive capabilities of these models require a better understanding the mechanical behavior of such metals [6]. Consecutively, techniques such as the out-of plane bulge and punch tests and in-plane cruciform tests are commonly used in the industry to investigate these effects[7-8]. However, both bulge tests and punch tests have significant limitations. For the punch test there are always bending and friction effects, which makes it a challenge to accurately predict the exact stresses and strains involved in the deformation process. For the bulge test there is no friction effect, bending however is still to be taken into account together. In addition, high pressures are needed if sheet metals are to be tested to fracture, which prevents miniaturization and severely complicate to the use of sensitive online microscopic diagnostics. It is also noted that in general out-of-plane deformation tests are more complicated to monitor with online full field measurements than in-plane tests. But most importantly, both punch and bulge test cannot be used to investigate complex strain paths[9].

Bhatnagar et al. [10] developed a new biaxial tensile testing fixture for loading an in-plane reinforced composite laminate in two principal directions. With advances in theoretical understanding, numerical capability, it is now possible to create fixtures that can allow us to predict the strength of materials under multiaxial loads. Experimental data however, still causes problem in comparison of theoretical data. Theoretical data is used for homogenized techniques that can be re-evaluated and compared repeatedly, thereby not allowing further study or understanding.

The present paper deals with the complete design of an innovative light weight fixture to be used in an 50kN UTM (table top: make Tenius Olsen) to conduct equibiaxial tension tests. Due to simple geometry of the fixture assembly, there is no pressure involved in this procedure. Hence, there is no

danger of explosions or uncontrolled fracture and necking propagation which occurs in other tests like Bulge Test. As the forces involved are tensile in nature, the results are more accurate and simple to calculate. The specimen is not in contact with any moving parts, hence there are no friction problems. The specimen of cruciform shape as per the standard undergoes strain purely due to pulling action of the fixture in two principal directions. There is no slip between specimen and jaws that hold it in place relative to the fixture assembly. The fixture distributes equal stress in both principal directions; however, the ratio of stress in the direction cannot be changed. Only equal stress in each direction can be carried out. Due consideration has been given to factor of safety to avoid the failure of fixture.

2. SPECIMEN DESIGN FOR BIAXIAL TEST

The cruciform type –[11] specimen design, as shown in Fig. 2, is selected for biaxial loading because it is simply gripped in the fixtures loading arms and hence eliminating the problems of friction and bending which are the main drawbacks of the Bulge test and punch draw tests. The another advantage of having cruciform type specimen is that stain can be easily measured in both the principal directions of loading which is not possible in punch tests. The extra fillet cut of 5mm are made at the corners of the specimen which reduces the stress concentration and help in transferring the load applied on the central part of the specimen, avoiding the failure of the arm under uniaxial loading.

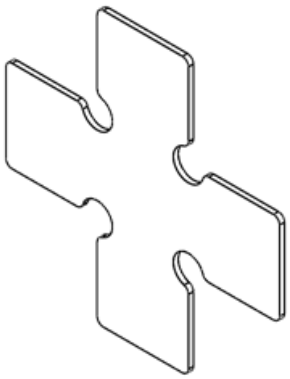

Fig. 2 Cruciform shaped specimen for biaxial tensile testing –[11]

3. DESIGN OF BIAXIAL TENSILE TESTING FIXTURE

The computer aided designed model of the fixture is shown in Fig. 3. The details of the various parts are given below:

The base (1) is a solid cylinder with three mountings on top to assemble the rod and the test plate holding jigs. The entire piece is made of high strength steel alloy. The upper frame (2) is the primary

component that distributes force in the fixture. Two arms at 30° angle to the vertical, and 60° angle between them. It is done so that the component of force in the horizontal direction on one arm is half of that applied in the vertical. Rod (3) are the members that connect the roller to the base. They also mount the slider. As there is no force being applied on the base, the vertical force on the upper frame gets distributed in both arms equally, and thus, a net equal force is obtained in the horizontal as well. Slots are cut into the arms to provide mounting for rollers . As the upper frame moves upwards, the rods rotate about their respective hinges such that the horizontal displacement is half of the vertical displacement. There is only a small section of the upper frame where this can happen. However, since the motion in the fixture will be very less due to the nature of the test plates, the motion will be sufficient for our purposes.

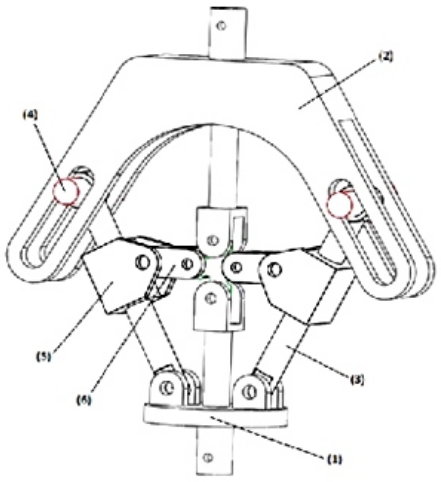

Fig. 3 A CAD model of the fixture showing different parts

Rollers (4) are the components that are mounted in the slots of the Upper Frame. They rotate in the slot to minimize sliding and prevent friction. They translate their motion. Sliders (5) are the components that mount the hinges. They have a cylindrical slot for the rod. They can slide about the rod. This gives leeway when setting up the fixture for an experiment. Hinges (6) are mounted in the Sliders using a pin. They swivel about the slider to help in setting up the experiment.

4. FINITE ELEMENT ANALYSIS

This fixture mechanism consists large number of components. Simulating such a system not only requires capturing the correct physical behavior but also using efficient techniques of analysis. Different levels of abstraction modeling are appropriate for separate stages of the design process. Kinematics and initial sizing can be studied using a partially rigid model, while final designs may be analyzed with completely meshed flexible geometry. Softwares used for CAE are Ansys Workbench 15.0 and Abaqus 6.11.

FEA consists mainly three stages which are described below briefly: Pre processing, Processing (Analysis) and Post processing .

The most important part of the analysis is to select a proper shape and number of element used to mesh the component. In the analysis of the fixture the shape of the element selected is Tetrahedon. Tetrahedron elements are used everywhere in the model for meshing. Each part of the assembly is meshed with fully integrated continuum 4-node C3D4 three- dimensional (3D) linear tetrahedron elements.

4.1 Loading and boundary conditions

The constrained in proper direction and of right type should be selected before applying the load. We have to tell the FEA package where we want to apply loads and where we want to constraint the part or assembly. We are assuming the factor of safety 2 for loading. we will operate the fixture at 50kN load so we are considering here 100 kN load. This tensile load is applied at top of the upper frame part. The bottom of the Base part is kept fixed. All the part or links of the fixture need to be constrained with the help different type of joints like cylindrical, spherical etc.

4.2 Linear Equation Solver Method

DIRECT SPARSE is the algorithm method used by the solver of Abaqus software by default to solve the linear equations. This solver extracts the solutions by solving multiple linear equations simultaneously with the help of matrices. Master stiffness equation is

$$\mathbf{Ku} = \mathbf{f}$$

Where **K** is the master stiffness matrix, **f** the vector of node forces and **u** the vector or node displacements. The equation is solved for deformations. Using the deflection values, stress, strain, and reactions are calculated. All the results can be used to plot graphic plots and charts.

For all the fixture components High Strength Steel is employed. Mechanical properties values of high strength steel is assigned, such as Young's modulus of 200 GPa, Poisson's ratio of 0.3, Yield tensile strength of 250MPa and Ultimate tensile strength of 460MPa.

The specimen material selected for simulation is aluminium1050. After the successful development and trial of the fixture we can test different materials including composites. Aluminium alloy AA1050 with mechanical properties as given below: Young's modulus=70 GPa, Poisson's ratio=0.33, Yield tensile strength=33MPa, Ultimate tensile strength=69MPa and these properties were determined experimentally in uniaxial tension test.

4.3 Kinematic simulation of fixture

The kinematic simulation of the fixture is by using MBD Module (rigid dynamic) in the ANSYS workbench 15.0. All the links were defined with respect to each other with the help of connectors. The displacement of right and left hinges was 2.57mm each when we provided a total displacement of 5mm to the upper frame. So the velocities in both the directions is same (97%) and error is just 2.8% which is quite tolerable in such experiments.

5. RAPID PROTOTYPING OF THE FIXTURE

Rapid Prototyping and Manufacturing (RP&M) technologies have emerged for quickly creating 3D products directly from computer-aided design systems. These technologies significantly improve the present prototyping practices in industries as well as for academic purposes. 3D printing is an additive manufacturing (AM), refers to various processes used to synthesize a three-dimensional object. In additive manufacturing processing, successive layers of material are formed under computer control to create the object. These objects can be of almost any shape or geometry and are produced from digital model data 3D model or another electronic data source.

5.1 The basic process of RP&M

A part is first modelled by a geometric modeler such as a solidworks modelling software. The part is then mathematically sectioned (sliced) into a series of parallel cross-section pieces. For each piece, the curing or binding paths are generated. These curing or binding paths are directly used to instruct the machine for producing the part by solidifying or binding a line of material. After a layer is built, a new layer is built on the previous one is the same way. Thus, the model is built layer by layer from the bottom to top. In summary, the rapid prototyping activities consist of two parts: data preparation and model production.

6. RESULTS AND DISCUSSIONS

The fixture is the master component and should be rigid while testing the specimens in equibiaxial tension, therefore the elastic deflection and the stress experienced by the components are designed to be the minimum. The stress contours in the fixture are shown in Fig. 4. The maximum values of stresses in the fixture components is 11 MPa & 6 MPa (shown in Fig.4) which are very well below the yielding stress of structural steel (250 MPa) selected in the design.

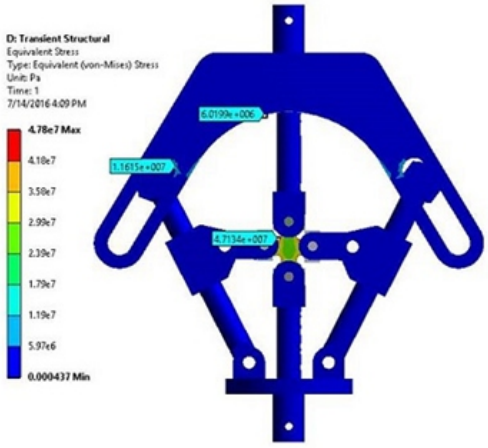

Fig. 4 Stress contours of the fixture after simulation

The stress contours of the specimen under equibiaxial tenson is shown in Fig. 5. In the specimen, the maximum equivalent Von-Mises stress value is 50 MPa (as shown in Fig. 5) which is above the yielding limit of Aluminium (33 MPa), depicting that the specimen has been yielded and is about to reach its UTS value or the state of instability. So All the deforming load is successfully transmitted to the testing specimen only and necking seems to occur at the region near the fillets of the specimen.

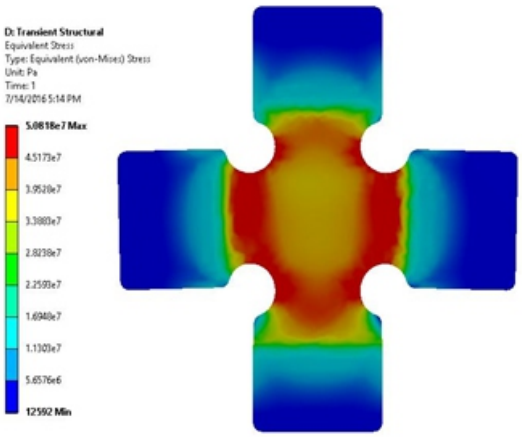

Fig. 7 Equivalent stress contours of the specimen under equibiaxial tension

From the results it is evident that there is no plastic strain in the components of biaxial fixture. All the load is transferred to the cruciform testing specimen and it undergone all the elastic as well as plastic deformation depending on the loading conditions. As we can see from the stress & strain contours the middle region is under biaxial stresses. And area shown in red color is most prominent to fracture.The maximum deformation causing elastic and plastic strain and stress in each part of the fixture as well as the specimen is given in table 1. The upper frame of the fixture which is connected to the moving head of the UTM experiences the maximum stress values and hence, the elastic deformation is maximum. The test specimen under equibiaxial load has been elongated by 3.063mm in both the primary directions resulting in necking at the center of the specimen.

Table 1 Simulation results

PARTS	MAX DEFORMATION (MM)	MAX VON MISES STRESS (MPA)
BASE	0.309	1.012
UPPER FRAME	0.407	1.261
ROD	0.072	0.171
SLIDER	0.092	0.972
HINGE	0.084	0.696
TEST SPECIMEN	3.063	4.785

7. CONCLUSIONS

On the basis of the finite element simulations of the fixture designed for equibiaxial tension only, the following conclusions can be drawn:

1. The design of the fixture is quite rigid and robust. The maximum values of Von-Mises stress in the fixture components are well below the yielding stress of structural steel selected in the design.
2. In the cruciform shaped specimen, the maximum equivalent Von-Mises stress value is 50 MPa which is well above the yielding limit of AA1050 aluminium alloy, depicting that the specimen has been yielded and is about to reach its UTS value or the state of instability. So All the deforming load is successfully transmitted to the testing specimen only and necking seems to occur at the region near the fillets of the specimen.

REFERENCES

1. Munera, D., Very and Ultra High Strength Steels Based Tailored Welded Blanks: A Step Further Towards Crashworthiness Improvement. SAE 2006 World Congress & Exhibition, 2006. ***2006-01-1213****.*

2. Xu, W., et al., Tensile and fatigue properties of fiber laser welded high strength low alloy and DP980 dual-phase steel joints. Materials & Design, 2013. ***43****: p. 373-383.*

3. Nakazima, K. and T. Kikuma, Forming limits under biaxial stretching of sheet metals. Testu-to Hagane, 1967. ***53****: p. 455-458.*

4. Keeler, S.P., Determination of forming limits in automotive stampings. 1965, SAE Technical Paper.

5. Holmberg, S., B. Enquist, and P. Thilderkvist, Evaluation of sheet metal formability by tensile tests. Journal of Materials Processing Technology, 2004. ***145****(1): p. 72-83.*

6. Kuwabara, T., A. Van Bael, and E. Iizuka, Measurement and analysis of yield locus and work hardening characteristics of steel sheets wtih different r-values. Acta Materialia, 2002. ***50****(14): p. 3717-3729.*

7. Ranta-Eskola, A.J., Use of the hydraulic bulge test in biaxial tensile testing. International Journal of Mechanical Sciences, 1979. ***21****(8): p. 457-465.*

8. Sowerby, R. and J.L. Duncan, Failure in sheet metal in biaxial tension. International Journal of Mechanical Sciences, 1971. ***13****(3): p. 217-229.*

9. Zang, S.L., et al., Prediction of anisotropy and hardening for metallic sheets in tension, simple shear and biaxial tension. International Journal of Mechanical Sciences, 2011. ***53****(5): p. 338-347.*

10. Bhatnagar, N., et al., Development of a biaxial tensile test fixture for reinforced thermoplastic composites. Polymer Testing, 2007. ***26****(2): p. 154-161.*

11. Geiger, M., W. Hußnätter, and M. Merklein, Specimen for a novel concept of the biaxial tension test. Journal of Materials Processing Technology, 2005. ***167****(2–3): p. 177-183.*

Design of Gear Train for Speed Magnification using the Cumulative Effect of Compounded Sun-Planet Gear Train

Sameen Mustafa[1‡], Ateeb Ahmad Khan[2]
[1]Department of Mechanical Engg., Faculty of Engg & Tech., Aligarh Muslim University, Student, C-10 Medical Colony AMU, sameenmustafa4@gmail.com,
[2]Department of Mechanical Engg., Faculty of Engg & Tech., Aligarh Muslim University, Asst. Professor, A-14 Medical Colony AMU , khanateebahmad@gmail.com
[‡]Corresponding Author; Tel: +91 7895702865

ABSTRACT

Designing a system in order to get high velocity ratios in gear trains has been a complex process since long time for design engineers. In this paper, this problem is solved and the authors are presenting the design of a gear train to get high velocity ratio which is further increased by compounding the developed design. The high velocity ratio is achieved by applying the concept of Sun-Planet gearing system. Authors have obtained a cumulative effect of speed of two gears on a single pinion, the driving gears being large and the pinion being small. The placement of two diametrically opposite gears for driving a single pinion generates a couple which doubles the velocity ratio transmitted to the pinion. Hence the resultant velocity ratio (ratio of output shaft speed to input shaft speed) increases as compared to a simple pair of two meshing gears.

Keywords- Velocity Ratio; gear train; gear; pinion; Sun-Planet gearing system.

1. INTRODUCTION

The Sun-Planet gearing system (Fig.1) consists of an array of gears arranged in such a way that the sun gear (driver) transmits equal motion (speed) to the planet gears (driven). This system increases the speed of the planet gears in equal proportions, but obtaining high velocity ratio in this case is difficult. In this research work, authors have reversed the role of the sun and the planets in the gearing system used. Authors have used two planet gears of large pitch diameter to drive the sun gear of small diameter (layout shown in Fig.2); such that the velocity ratio imparted to the sun is twice that of a single pair of gear and pinion.

Considerable amount of research work has been carried out to obtain good velocity ratios in gear trains. Jose M. del Castillo [2] presented two procedures for finding efficiency of a PGT. They presented that the analytical expression for the efficiency could be expressed in terms of the output speed ratio and the virtual gear teeth ratio. They concluded that by knowing the output speed ratio one can determine efficiency of the PGT.

G Mantriota [1] carried out a kinetic study on a PS-CVT system to obtain output power larger than that circulating in the CVT. They proposed a solution to allow an input power in the CVT less than that of the output power of the PS-CVT. It was concluded that it is possible to improve the efficiency of the high transmission ratios compared with the simple CVT. Thus they provided a solution for applications having an elevated transmission ratio.

D. Mundo [3] investigated the mechanical configuration of a typical planetary drive. They determined the gear ratio law for four possible configurations of a planetary drive considering a single degree of freedom mechanism. They presented a planetary gear train with non circular gears as a mechanism for riding bicycles. It was concluded that the device can improve the cyclist's performance for a low speed way of pedaling.

D C. Talbot et. al [4] presented a database of mechanical and spin power losses in a planetary gear set and lubricant. They showed that changing the number of planets of a planetary gear set is not a feasible way of changing the gear set efficiency. It was also proved that gear sets having smoother tooth surfaces provided reduced mechanical power loss.

Tianli Xie et. al [5] presented a methodology for design of seven speed PGTs, which was used to the serial design of PGT products which could spread over a wide range starting from passenger vehicles to the military vehicles.

Fuchun Yang et. al [6] studied a method based on hyper graph and matrix operations for estimation of velocity, torque and power flow analyses of MFPGT systems. They proved that these methods were feasible and efficient for those analyses. They also showed that partial shafts might bear self locking when the efficiency of the system is positive and that the characteristic parameters of SPGTs could affect the efficiency of the gearing system.

2. EXPERIMENTAL SETUP AND WORKING

The experimental setup consists of a total of two spur gear trains (having three gears each) arranged in parallel (Fig. 3). The setup comprises of the following:

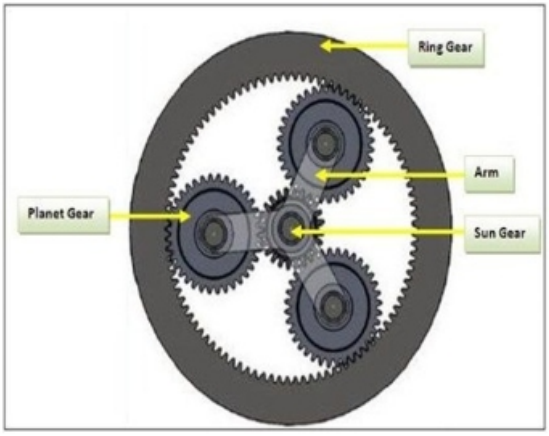

Figure 1: A typical Sun-Planet gear

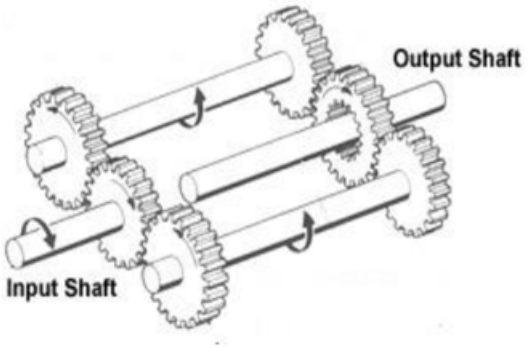

Figure 2: Layout showing the concept used in this work.

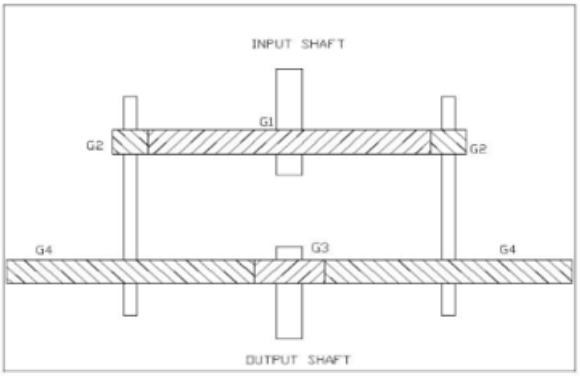

Figure 3: Schematic diagram showing the design of the compounded gearing system.

$\sum 1^{st}$ train comprising of a gear of 32" pitch diameter and two pinions of 4"

diameters represented by G1 and G2 respectively.

$\sum 2^{nd}$ train comprising of two pinions of 28" pitch diameters and a gear of 8" diameter represented by G3 and G4 respectively.

Velocity Ratio achieved in the 1st gear train is 8:1 such that each of the planet gears rotate with eight times the speed of the sun. The pinions from the 1st gear train transmit the same speed to the gears of the 2nd train; each planet gear in this train imparts the VR of 3.5:1 to the pinion, as a result of which a cumulative VR of 7:1 (3.5*2) is obtained. Thus at the end of the gearing system a high speed is provided to the counter shaft which 56 times greater than the speed of the input shaft.

3. FORMULA AND SYMBOLS USED

d1= pitch diameter of gear
d2= pitch diameter of pinion
N1= speed of gear in rpm
N2= speed of pinion in rpm
VR= velocity ratio

$$VR = \frac{Speed\ of\ pinion}{Speed\ of\ gear} = \frac{N2}{N1}$$

$$VR = \frac{pitch\ diameter\ of\ gear}{pitch\ diameter\ of\ pinion} = \frac{d1}{d2}$$

4. RESULTS AND DISCUSSIONS

Experimental tests were performed at an input speed of 2rpm. The velocity ratios obtained for each pair of meshing gear is shown in Table 1. The two planet gears (G2) rotate with a speed of 16rpm which is transmitted by means of shafts to the two G4 gears. These gears now drive the sun gear (G3) at a speed of 112rpm. It can be seen from the results obtained that the output speed has been magnified considerably in two steps only.

Fig.4 shows that unlike the traditional processes of procuring good velocity ratios in gear trains, our experimental procedure increases the output speed exponentially. Hence the complexity in compounding gear trains to achieve the same velocity ratio can be wiped out using this configuration of gears. It can be observed from Fig.5 that the velocity ratios obtained by the compounded sun-planet gearing system are excellent as compared to that of a normal gear train.

Gear	Speed (rpm)	Velocity Ratio	Overall VR
G1	2	8:01	8:01
G2	16		
G3	112	7:01	56:01:00
G4	16		

Table 1: table showing gears and their VRs

Compounding stage	Normal VR	Compounded VR
Stage 1	8:01	8:01
Stage 2	3.5:1	7:01
Output	28:01:00	56:01:00

Table 2: Comparison between normal gear train and designed gear train

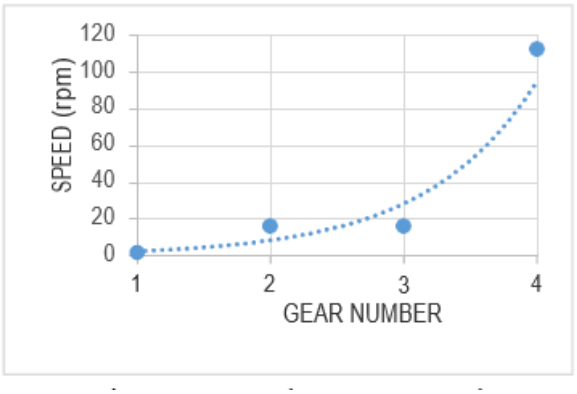

Figure 4: Speed vs. Gear Used

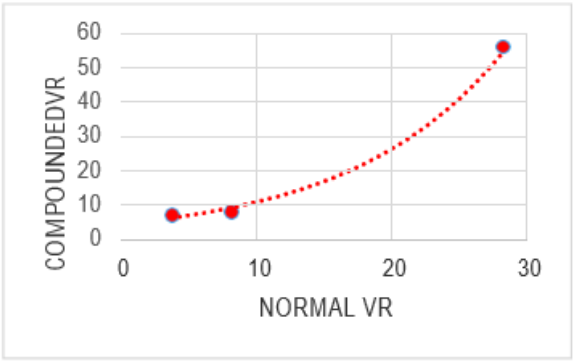

Figure 5: Compounded VR vs. Normal VR

5. CONCLUSION

The developed design of the gearing system presented in this paper to achieve high velocity ratio is an efficacious design whose effect is magnified substantially by compounding. This research shows that with the two step compounding, authors have acheived a velocity ratio of as high as 56:1. The compounding stages can further be increased to get even higher velocity ratio, if required.

Future aspect: With this developed design of compounded sun-planet gearing system the possibilities of obtaining high speeds are endless if the judicious compounding of the sun-planet gearing system is maintained. Velocity ratio of about 1600:1 is achievable in only two steps of compounding the designed gear train. Thus even if the input speed is 1rpm, the output speed will be sufficient to drive alternators and generators, pump water to greater heights and drive flour mills and other useful equipments in urban areas. Hence the scope of this design is vast and its applications are numerous.

6. REFERENCES

[1] G Mantriota, Power split continuously variable transmission systems with high efficiency, Proc Instn Mech Engrs, 2000, Vol. 215 Part D.

[2] Jose M. del Castillo, The analytical expression of the efficiency of planetary gear trains, Mechanism and Machine Theory, 2001, vol. 36, pp. 197-214.

[3] D. Mundo, Geometric design of a planetary gear train with non-circular gears, Mechanism and Machine Theory, 2005, vol. 41, pp. 456-472.

[4] D C. Talbot, A Kahraman, A Singh, An Experimental Investigation of the Efficiency of Planetary Gear Sets, Journal of Mechanical Design, 2012, vol. 134, DOI:10.1115/1.4005599.

[5] Tianli Xie, J Hu, Z Peng and C Liu, Synthesis of seven-speed planetary gear trains for heavy-duty commercial vehicles, Mechanism and Machine Theory, 2014, vol. 90, pp. 230-239.

[6] Fuchun Yang, J Feng and H Zhang, Power flow and efficiency analysis of multi-flow planetary gear trains, Mechanism and Machine Theory, 2015, vol. 92, pp.86-89.

Development of Polynomials for the Thermodynamic Properties of Refrigerant R-134a.

Aseem Dubey
Krishna Institute of Engineering and Technology, Ghaziabad, UP, India
Email ID- aseemdubey009@gmail.com
Mobile- +918585909217

A B S T R A C T

The polynomials have been developed to evaluate the thermodynamic properties of Refrigerant R-134a. They are more accurate, simple and computationally faster. The accuracy of the calculated results obtained are within the admissibility with deviation between 0.01% to 0.6% and found to be much closer as compared with source data (experimental) for a given temperature range of temperature (i.e. 40° C to 50° C), reported in publications. This level of accuracy of the properties, evaluated from the developed equations may be used in various applications, such as dynamic simulations of performance of refrigeration systems, capillary tube design etc.

Keywords: Thermodynamic Properties, Polynomials, Refrigerant R-134a

1. INTRODUCTION

The use of refrigerant R-134a in refrigerating equipment fully abides by the rules of the Montreal Protocol, which puts the restriction on the use of ozone distorting chlorofluoro carbons (CFCs). There are a number of possible substitute fluids that contain one or more hydrogen atoms and as a result, have shorter atmospheric lifetimes than the CFCs. In particular, R-134a is found to be as a replacement of refrigerant R-12 due to low ozone depletion potential.

With the development of new refrigerants there is a need to develop correlations in the form of curve - fits polynomials for new refrigerants. A difficulty in this is that the measurement of thermodynamic properties of these refrigerants proposed by various researchers is far from complete agreement. Experimental values are proposed [1, 2, 3] which differs from each other. Measurements and formulation of thermodynamic properties [4] has also being carried out by many researchers. Cleland [5] has developed polynomial curve - fits for R-134a. Hou et al. [6] carried out experimental study of density and viscosity of compressed R-134a. Shankland et al. has researched the Thermal conductivity and viscosity of new stratospherically safe Refrigerant R-134a.

In order to use the thermodynamic properties of R134a for various applications such as, dynamic simulations of performance of refrigeration systems, capillary tube design etc. polynomials have been developed. The proposed polynomials are simpler and computationally fast to evaluate thermodynamic properties of Refrigerant R-134a in liquid and vapor phase, with a reasonable accuracy 0.6%, which is helpful to carry out many research activities related to dynamic simulation of refrigeration system. The properties thus obtained have been compared with experimental values [4, 6, 7] and standard values published by SRF Ltd. for a temperature range – 40°C to 50°C which is normally encountered in practice for practical applications. The main requirements of these polynomials are to calculate;

a. Vapor pressure from saturation temperature.
b. Liquid density from saturation temperature.
c. Vapor density from saturation temperature.
d. Liquid enthalpy from saturation temperature.
e. Vapor enthalpy from saturation temperature.
f. Liquid entropy from saturation temperature.
g. Vapor entropy from saturation temperature.
h. Liquid viscosity from saturation temperature.
i. Vapor viscosity from saturation temperature.
j. Specific heat of vapor at constant pressure against temperature.

2. STATISTICAL ANALYSIS

The polynomial equations can be fitted between various pairs of variables to study the thermodynamic properties with the help of experimental data and using the method of least squares. In general the equation of the curve can be represented by a polynomial equation of order 'p' between the variables E an T as follows:

$$E = a + bT + CT^{2} + - - nT^{p} \qquad (1)$$

Where a, b … n are constants

To determine the value of these constants the equation is to be differentiated partially w. rt. a, b …, n so as to minimize the sum of the squares due to error. This yields the following equations:

$$\begin{aligned} \Sigma E &= Na + b\Sigma T + c\Sigma T^2 + d\Sigma T^3 \\ \Sigma TE &= a\Sigma T + b\Sigma T^2 + c\Sigma T^3 + d\Sigma T^4 \\ \Sigma T^2E &= a\Sigma T^2 + b\Sigma T^3 + c\Sigma T^4 + d\Sigma T^5 \\ \Sigma T^3E &= a\Sigma T^3 + b\Sigma T^4 + c\Sigma T^5 + d\Sigma T^6 \end{aligned}$$

Where |

N = Number of paired observations

3. PROPERTIES CORRELATIONS

With the help of mathematical analysis a computer program in MAT-Lab has been developed to obtain the correlation of following thermodynamic properties.

3.1 Vapor Pressure

The pressure of vapor is dependent on saturation temperature. The polynomial curve - fits are as follows;

$$P = a_1 + a_2 T_{sat} + a_3 T^2_{sat} + a_4 T^3_{sat} \qquad (2)$$

The temperature range of the applicability of this polynomial is $-40^{\circ}C \leq T_{sat} \leq 60^{\circ}C$. Across this range the difference occurs from 0.002% to 0.6% as compared with source data.

3.2 Liquid Density

The polynomial curve - fits to calculate liquid density at a given temperature (T_f) is expressed as;

$$\rho_f = b_1 + b_2 T_f + b_3 T_f^2 + b_4 T_f^3 \qquad (3)$$

The temperature range of the applicability of this curve - fits is $-40^{\circ}C \leq T_f \leq 60^{\circ}C$. Across the full range of applicability the largest difference of liquid density occurs 0.60% at $30^{\circ}C$. However, this difference is narrowed down to 0.002% for other temperature as compared with source data.

3.3 Vapor Density

The saturated vapor densities of refrigerant are fits in the following form

$$ln\rho_g = c_1 + c_2 T_{sat} + c_3 T_{sat}^2 + c_4 T_{sat}^3 \qquad (4)$$

The temperature range of the applicability of this curve fits is $-40^{\circ} C \leq T_{sat} \leq 50^{\circ} C$. Across the full range of applicability the largest difference occurs from 0.01% to 0.35% for other temperature as compared with source data.

3.4 Liquid Enthalpy

The enthalpy of liquid refrigerant is virtually independent of the pressure over it. The curve - fit Polynomial for liquid enthalpy at a given temperature (T_f) and using ASHRAE Reference condition is given as follows:

$$h_f = d_1 + d_2 T_f + d_3 T_f^2 \qquad (5)$$

The temperature range of the applicability of this curve - fits is -40^o C $\leq T_f \leq 60^o$ C. Across the full range of applicability the highest difference occur 0.52% at -30^o C. For other temperature range the largest difference occurs upto 0.01% as compared with source data.

3.5 Vapor Enthalpy

A second order polynomial is an adequate predictor for calculating saturated vapor enthalpy from saturation temperature. Using ASHRAE reference conditions the vapor enthalpy is expressed in the following form;

$$h_g = e_1 + e_2 T_{sat} + e_3 T_{sat}^2 \qquad (6)$$

The temperature range of the applicability of this polynomial is -40^o C $\leq T_{sat}$ 60^o C. The largest difference occurs from 0.25% at 30^o C. For other temperature range this difference occurs upto 0.01% as compared with source data.

3.6 Liquid Entropy

The polynomial curve fit to calculate the liquid entropy at a given temperature (T_f) is expressed as follow:

$$s_f = f_1 + f_2 T_f + f_3 T_f^2 \qquad (7)$$

The temperature range of the applicability of this polynomial is -40^o C $T_f \leq 60^o$ C. The largest difference occurs 0.01% for full range of temperature as compared with source data.

3.7 Vapor Entropy

The polynomial curve fits to calculate vapour density against saturation temperature is expressed as:

$$s_g = g_1 + g_2 T_{sat} + g_3 T_{sat}^2 \qquad (8)$$

The temperature range of the applicability of this polynomial is -40^o C $\leq T_{sat}$ 60^o C. The largest difference for this temperature range occurs to be 0.55% as compared with experimental data.

3.8 Liquid Viscosity

The third order curve fill for liquid viscosity against temperature (T_f) is expressed as;

$$_f = h_1 + h_2 T_f + h_3 T_f^2 + h_4 T_f^3 \qquad (9)$$

The temperature range of the applicability of this polynomial is – 40° C £ T_f 50° C. The largest difference occurs is 0.60% at 50° C. For other temperature range the difference occurs upto 0.15% as compared with experimental data.

3.9 Vapour Viscosity

The third order polynomial curve fits for vapor viscosity against temperature (T_{sat}) is expressed as;

$$_g = j_1 + j_2 T_{sat} + j_3 Ts_{at}^{\ 2} + j_4 T_{sat}^{\ 3} \qquad (10)$$

The temperature range of the applicability of this polynomial is – 40° C £ T_{sat} 50° C. For full range of temperature the difference occurs is less than 0.6% as compared with experimental data.

3.10 Specific Heat of Vapor

The curve fits polynomial for specific heat of vapor at constant pressure against temperature in expressed as

$$C_p = k_1 + k_2 T_{sat} + k_3 T_{sat}^{\ 2} + k_4 T^3_{sat} \qquad (3.11)$$

The temperature range of the applicability of this polynomial is lies between – 40° C T_{sat} 50° C. The largest difference occurs is 0.6% at 50° C. For other temperature the largest difference occurs 0.3% as compared with source data.

Viscosity of liquid refrigerant is a controlling factor for applications due to its large numerical values compared with viscosity of vapor. As the temperature lower down, the magnitude of the viscosity of liquid refrigerant increases of that vapor decreases. Using the property correlation developed the variation of viscosity of refrigerant R134a in liquid and vapor phase with respect to temperature has been plotted in the form of graph and shown in Figure 1.

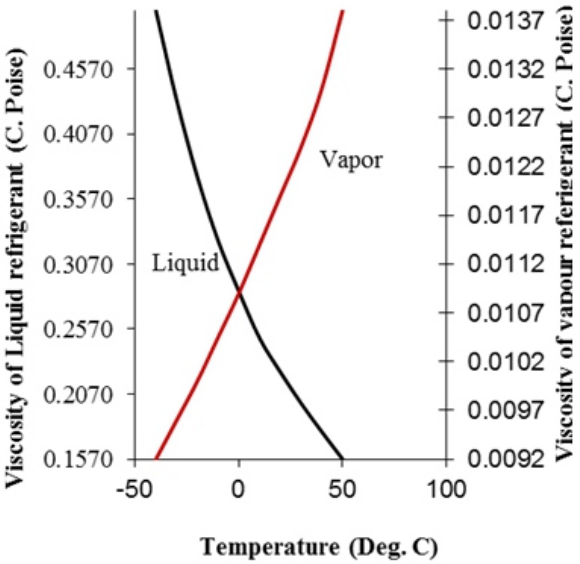

Figure 1. Variation of Liquid and Vapor viscosity with Temperature

Table 1 gives the values of different constants of curve fit polynomials evaluated

Table 1. Coefficients for the Equations

a_1 = 2.9258844	f_1= 0.1929074
a_2 = 0.10615557	f_2= 4.7977881 E-3
a_3 = 1.5099567 E-3	f_3= -4.6957781 E-7
a_4 = 9.0488214 E-6	g_1= 0.9192099
b_1= 1292.257	g_2= -7.1935853 E-4
b_2= -3.2541661	g_3= 6.1000277 E-6
b_3= -7.3214283 E-3	h_1= 0.2865833
b_4= -5.2083333 E-5	h_2= -3.66 E-3
c_1= 2.667350876	h_3= 3.3996484 E-5
c_2= 0.03507896	h_4= -2.4375312 E-7
c_3= -1.235192 E-4	j_1= 0.010966857
c_4= 6.0702243 E-7	j_2= 4.4607638 E-5
d_1= 49.1037624	j_3= 1.3392857 E-7
d_2= 1.32231629	j_4= 2.7517361 E-9
d_3= 2.3908840 E-3	k_1= 0.8921428
e_1= 247.6867293	k_2= 4.416666 E-3
e_2= 0.5603172	k_3= 2.98211428 E-5
e_3= -1.276252 E-3	k_4=2.708333 E-7

4. CONCLUSION

The curve - fit equations reduce the computational time required for evaluation of thermodynamic properties of refrigerant R-134a. They are sufficiently accurate across the temperature a range specified and gives satisfactory performance. These proposed equations are in the simplest form known to the authors so far and a percentage error is within a reasonable range (0.6 %) and occurs occasionally. The errors may be due to due to the available thermodynamic data for R-134a are sparse and probably not as precise as for other refrigerants. These polynomial curve fits can be used well for dynamic simulation of refrigeration system to achieve a satisfactory performance for a temperature range – 40° C to 50° C (233K– 323K).

Nomenclature

C_p = Specific heat of vapor (KJ/kg K)
h_f = Enthalpy of saturated liquid KJ/Kg)
h = Enthalpy of saturated vapor (KJ/Kg)
P = Pressure (Bar)
s_f = Entropy of saturated liquid (KJ/Kg K)
s_g = Entropy of saturated vapor (KJ/Kg K)
T = Temperature (°C)
ρ_f = Saturated liquid density (Kg/m^3)
ρ_g = Saturated vapor density (Kg/m^3)
μ_f = Dynamic viscosity of liquid (centi. poise)
μ_g = Dynamic viscosity of vapor (centi. poise)

Subscript

f =Liquid state
g =Gaseous or vapor state
Sat =Saturation

5. REFERENCES

[1] A.C. Cleland, "Computer sub-routines for rapid evaluation of refrigerant thermodynamic properties", Int. J. Refrigeration, 1986, Vol. 9, pp. 346-351.

[2] J.W. Magee, and J.B. Howley, "Vapor pressure measurements on 1, 1, 1, 2 – tetrafluoromethane (R-134a) from 180 to 350 K", Int. J. Refrigeration, 1992, Vol. 15, pp. 386-392.

[3] M.L. Huber, and J.F. Ely, "An equation of state formulation of thermodynamic properties of R-134a", Int. J. Refrigeration, 1992, Vol.15, pp. 393-400.

[4] M.O. Mc Linden J.S. Gallaghar, L. A. Weber, G. Morrision, D. Ward, A. R. H. Goodwin, M. R. MoldoverJ. W. Schmidt, H. B. Chae, T. J. Bruno, J. F. Ely, and M. L. Huber, "Measurement and formulation of the thermodynamic properties of refrigerant R-134a and R-123", ASHRAE Trans, Vol. 92, pp. 263-283, 1989.

[5] A.C. Cleland, "Polynomial curve fits for refrigerant thermodynamic properties: extension to include R-134a", Int. J. Refrigeration, 1994, Vol. 17, pp. 245-249.

[6] H. Hou, J.C. Holte, B. E. Gammon, and K. N. Marsh, "Experimental densities for compressed R-134a", Int. J. Refrigeration., 1992, Vol. 15 (6), pp. 365-371.

[7] Shankland, R. S. Basu, and D. P. Wilson, "Thermal conductivity and viscosity of new stratospherically safe Refrigerant - 1, 1, 1, 2-Tetrafluoroethane (R-134A)", CFCs: Time of Trans. Altanta, Georgia: ASHRAE, pp. 117-122, 1989.

Effect of Diethyl Ether and Biodiesel Blend on the Performance and Emissions from a Diesel Engine

Mohit kumar[‡1], Shashank Mohan[1]andAmit Pal[1],

[1].Mechanical Engineering Department, Delhi Technological University, Bawana Road, Delhi-110042,

mohitofficialid@gmail.com,

A B S T R A C T

The goal of this study was to evaluate the performance and emission characteristics of diesel engine using oxygenated fuels (blending agents). In view of this, experimental investigations were carried out on a single cylinder four stroke direct injection water-cooled diesel engine using biodiesel (B) of waste cooking oil and diethyl ether (DEE) blended fuels in different volume ratios with diesel fuel. The investigation was performed with four different blends (B0DEE0D100, B10DEE10D80, B20DEE20D60&B0DEE20D80) to assess the impact of using biodiesel and diethyl ether-diesel blends on diesel engine performance and emissions. No emulsifier was needed for blend to retain homogeneity and prevent the interfacial tension between two liquids in case of DEE. For the same rated speed and compression ratio, different blended fuels as well as pure diesel, various engine parameters such as brake thermal efficiency, brake specific energy consumption, brake specific fuel consumption, exhaust gas temperature and exhaust emissions such as smoke opacity, hydrocarbon, CO,CO_2 and NOx, were measured. The results indicate that the brake thermal efficiency was increased with an increase in biodiesel and DEE contents in the blended fuels and break specific fuel consumption and break specific energy consumption being almost same for all fuel blends at overall operating conditions. At higher loads, reduced CO emission levels were observed for blends of biodiesel and DEE at high load. HC emissions increased for all blends of biodiesel and DEE compared with diesel and NOx emission slightly reduced with biodiesel and DEE blends compared to diesel at lower loads.

KEYWORDS: Renewable fuels, Diethyl Ether, waste cooking oil, brake thermal efficiency, nitrogen oxides and emissions

1. INTRODUCTION

Diesel engines are the most popular well known efficient prime mover among the internal combustion engines because of their simple, robust construction coupled with high thermal efficiency and specific power output with better fuel economy, much longer life span and reliability which results in their wide spread use in transportation, thermal power generation and many more industrial and agricultural applications. Inspite of many advantages, the diesel engine is inherently dirty and is the most significant contributor of various air polluting exhaust gases such as particulate matter (PM), oxides of nitrogen (NOx), carbon monoxide (CO) and other harmful compounds which contribute to serious public health problems. Particulate matter (PM) emissions from diesel combustion contribute to urban and regional

Diesel engines are the most popular well known efficient prime mover among the internal combustion engines because of their simple, robust construction coupled with high thermal efficiency and specific power output with better fuel economy, much longer life span and reliability which results in their wide spread use in transportation, thermal power generation and many more industrial and agricultural applications. Inspite of many advantages, the diesel engine is inherently dirty and is the most significant contributor of various air polluting exhaust gases such as particulate matter (PM), oxides of nitrogen (NOx), carbon monoxide (CO) and other harmful compounds which contribute to serious public health problems. Particulate matter (PM) emissions from diesel combustion contribute to urban and regional hazes. Nitrogen oxides (NOx) and hydrocarbons (HC) are precursors for O_3 and PM. NOx emissions from diesel vehicles play a major role in ground-level ozone formation. Ozone is a lung and respiratory irritant causes a range of health problems related to breathing, including chest pain, coughing and shortness of breath. Particulate matter has been linked to premature death, and increased respiratory symptoms and disease. In addition, ozone, NO, and particulate matter adversely affect the environment in various ways, including crop damage, acid rain and visibility impairment.

In view of increased concerns regarding the effects of diesel engine particulate and NOx emissions on human health and the environment and more stringent government regulation on exhaust emissions, reducing the NOx and particulate emission from diesel engines is one of the most significant challenges. The rapid depletion, uneven distribution of petroleum fuels, their ever increasing costs and great concern over pollution led to search for an alternative fuel to replace conventional fuels. The most promising alternative possibility to clear this critical issue is to use the oxygenated fuels either in pure form or blended with diesel to provide sufficient oxygen and promote combustion and reducing PM emission and possibly decreasing NOx emission.

Oxygenated fuels are the attractive class of synthetic fuels in which Oxygen atoms are chemically bound within the fuel structure. This Oxygen bond in the oxygenated fuel is energetic and provides a chemical energy that result in no loss of efficiency during combustion. The optimization of oxygenated fuels, to be used either as, neat fuel or as an additive, offers significant potential for reduction in particulate emission. In this study, two oxygenates are tested with diesel in blended form to investigate the performance, combustion and emissions of a diesel engine.

Property	Diesel	Dimethyl Ether	Diethyl Ether	Biodiesel
Boiling point ^{0}C	146-374	-25	34.44	182-337
Cetane number	40-55	>55	>125	46-55
Autoignition temperature ^{0}C	315	350	160	373-448
Flash point^{0}C	56-75	-41	-45	165
Stoichiometric Air/fuel Ratio	15	8.9	11.1	13.8
Lower heating Value, kJ/kg	43000	28191.12	35400.14	37500
Kinematic Viscosity @40 ^{0}C cSt	3.2	-	0.24	4.5
Density , kg/L	820-950	713	714	815-890
Energy Density (MJ/L)	35.8	19.3	20.6	23.4

Table 1. Comparison of properties of potential CI engine fuel components[3,6,14]

Diethyl ether, also known as ethoxy ethane, ethyl ether, sulfuric ether, or simply ether, is an organic compound in the ether class with the formula $(C_2H_5)_2O$. It is a colorless, highly volatile, flammable liquid produced as a byproduct of the vapor-phase hydration of ethylene to make ethanol. Diethyl ether has a high cetane number of 85-96 and is used as a starting fluid, in combination with petroleum distillates for gasoline and diesel engines, due to its high volatility and low flashpoint.

DEE has long been known as a cold-start aid for engines, but little is known about using DEE as a significant component in a blend or as a complete replacement for diesel fuel or biodiesel. To identify the potential of DEE as transportation fuel a comprehensive literature review was carried out by Baily et al. [7]

Many researchers have conducted experimental investigation on the diesel engines fuelled with diesel blended fuels. Some of those are briefly highlighted in the following section.

Geo et al. [1] found that thermal efficiency of the engine was improved from 26.5% with neat Rubber Seed Oil to a most of 28.5% with DEE injection rate of 200 g/h. Smoke was reduced from 6.1 to 4 BSU with DEE injection at the maximum efficiency flow rate. Hydrocarbon and carbon monoxide gas emissions were also less with DEE injection. Sivalakshmi and Balusamy [2] concluded that the addition of diethyl ether into biodiesel improved the physicochemical properties of biodiesel. Smoke emissions were found lower and HC &NOx emission was higher for BD5 compared to that of neat biodiesel. Hence, they reported that addition of diethyl ether up to 5% (by vol.) would be a promising technique for using biodiesel efficiently in diesel engines with none modifications in the engine. Sezer [3] investigated the use of dimethyl ether and diethyl ether in diesel engines as alternative fuels. Engine performance for dimethyl ether and diethyl ether was extensively improved for the same equivalence ratio condition, but a more amount of fuel was needed about 64% for dimethyl ether and 32% for diethyl ether. In the experiments of Ashok and Saravanan [4] the oxygenated additive diethyl ether was added on a 10th by volume basis along with the emulsified fuel 70D:30E. They found that Use of emulsified fuel increases the brake thermal efficiency and reduces the specific fuel consumption, smoke density, and particulate matter with much rising of NOx. But Addition of diethyl ether to the emulsified fuel improved the performance and reduces the emissions, NOx and ignition delay. Phan and Phan [5]carried out alkali-catalysed trans-esterification of waste cooking oils, collected within Ho Chi Minh City, Vietnam, with methyl alcohol in a laboratory scale reactor and revealed that the biodiesel experienced a higher but much narrower boiling range than conventional diesel& there was little variation in properties among the WCO samples in terms of chemical and physical properties. Banapurmath et al. [6] did experiments using ethyl alcohol and diethyl ether blended fuels in distinct volume ratios with diesel fuel. DEE-diesel blends showed lower emissions compared to ethyl alcohol-

diesel blends. Ali et al. [8] blended an oxygenated additive diethyl ether (DEE) with palm oil biodiesel (POME) in the ratios of 2%, 4%, 6% and 8% and tested for their properties improvement to characterize how the key fuel properties changed when diethyl ether were blended with palm oil methyl esters. Iranmanesh et al. [9] showed that the 5% DEE-Diesel fuel and 15% DEE-Biodiesel blend were the optimal blend based on performance and emission characteristics.

Lapuerta et al. [10] tested two different alcohol-derived biodiesel fuels: methyl ester and ethyl ester, both obtained from waste cooking oil. These biodiesel fuels were tested pure and blended (30% and 70% biodiesel content, volume basis) with a diesel reference fuel, which was tested too, in a common-rail injection diesel engine and thus the type of alcohol used in the production process was found to have a significant effect on the total hydrocarbon emissions and on the particulate matter composition. Zhang et al. [11]revealed that Brake-specific fuel consumption of biodiesel-diesel-DEE blends increases with the increase of oxygenated-fuel fraction in these blends. Brake thermal efficiency exhibits minimal variation when operating on different biodiesel-diesel-DEE blends. NOx emission increases with increasing biodiesel fraction in the diesel-biodiesel-DEE blends at medium load and at high load but Particle mass and HC and CO emissions decrease with the increase of oxygenated fuel fraction in the blends. Zhang et al. [12] developed four different continuous process flow-sheets for biodiesel production from virgin vegetable oil or waste cooking oil under alkaline or acidic conditions on a commercial scale. Detailed operating conditions and equipment designs for each process were obtained. The acid-catalyzed process using waste cooking oil proved to be technically feasible with less complexity than the alkali-catalyzed process using waste cooking oil, thereby making it a competitive alternative to commercial biodiesel production by the alkali-catalyzed process and The alkali-catalyzed process using virgin vegetable oil as the raw material required the fewest and smallest process equipment units but at a higher raw material cost than the other processes. Sivalakshmi and Balusamy [13] observed effects of diethyl ether and ethanol as additives to biodiesel (neem oil methyl ester NOME) on the performance and emission characteristics of a diesel engine at different loads and constant engine speed. Compared with biodiesel, slightly lower brake specific energy consumption for diethyl ether and ethanol blended biodiesel fuels was observed. At higher engine loads, CO and smoke emissions were found significantly lower with all blends. Patil and Thipse [14] showed that DEE can be mixed in any proportion in diesel and kerosene as it is completely miscible with diesel fuel. The density, kinematic viscosity and calorific value of the blends decreased while the oxygen content and cetane number of the blends increased with the concentration of DEE in the blends. Sachuthananthan and Jeyachandran[15] found that DEE when added to water-biodiesel emulsion can significantly lower NOx and smoke levels without adverse effect on brake thermal efficiency. High HC and high CO, which are problems with the water-biodiesel emulsions, can be significantly lowered with the addition of DEE particularly at high outputs.

In the present work, the purpose of this investigation is to study the effect of DEE and biodiesel (WCO) as a supplementary oxygenated fuel with high speed diesel fuel (HSD as baseline fuels on the simultaneous reduction of NOx and smoke emissions. It is also desired to find out optimum blend with diesel fuel on the basis of performance and emissions characteristics.

2. EXPERIMENTAL SETUP

The setup consists of single cylinder, four strokes, Multi-fuel, research Engine connected to eddy current type dynamometer for loading. Instruments are provided to interface airflow, fuel flow, temperatures and load measurements. The setup has stand-alone panel box consisting of air box, two fuel tanks for duel fuel test, manometer, fuel measuring unit, transmitters for air and fuel flow measurements, process indicator and hardware interface. Rotameters are provided for cooling water and Calorimeter water flow measurement. The main engine specifications are: bore 80 mm, stroke 110 mm, compression ratio 17.5, maximum power 3.5 kW at 1500 rev/min. Engine speed and load are controlled by varying excitation current to the eddy current dynamometer using dynamometer controller. An AVL exhaust gas analyzer (Model: diGas 444) and AVL Smoke meter (Model: 437) are used to measure emission parameters CO, HC, and NOx and smoke intensity respectively.

1-Control Panel, 2-Computer system, 3-Diesel flow line, 4-Air flow line,5-Calorimeter, 6-Exhaust gas analyzer, 7-Smoke meter, 8-Rota meter, 9,11-Inlet water temperature, 10-Calorimeter inlet water temperature,12-Calorimeter outlet water temperature, 13-Dynamometer, 14-CI Engine, 15-Speed measurement, 16-Burette for fuel measurement, 17-Exhaust gasoutlet, 18-Outlet water temperature, T1-Inlet water temperature, T2-Outletwater temperature, T3-Exhaust gas temperature.

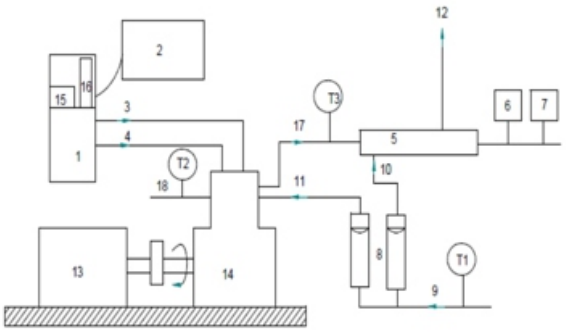

Fig. 1. Kirloskar diesel engine test set up

Loads are changed in five levels from no load to the maximum load. The engine is operated at the rated speed i.e., 1500 rev/min for all the tests. For each load condition, the engine was run for at least 5 minutes after which data was collected.

Fuel formulations were made with addition of diethyl ether and biodiesel (from Waste cooking oil) as supplementary fuels to the high speed diesel fuel (HSD). DEE and WCO biodiesel were blended with HSD as B10DEE10D80, B20DEE20D60 &B0DEE20D80.The observations made during the test for the determination of various engine parameters included brake load, engine speed, time for fuel blends consumption, drop in air pressure across the orifice of the air-stabilizing tank, exhaust gas temperature and exhaust emissions.

Table 2. Properties of test fuels

Fuel	Density (g/ml)	LCV (kJ/kg)	Cetane number
DIESEL(D)	0.832	43000	48
B10DEE10D80	0.825	41680	56
B20DEE20D60	0.818	40360	65
B0DEE20D80	0.808	41460	63

3. RESULT AND DISCUSSIONS

Performance characteristics

Fig. 2 represents the variation of brake specific fuel consumption with brake power for different fuels. The BSFC is high at low load for all the fuels and as we increase the load the BSFC start decreasing, this trend follows approximately up to 50% to 70% load and if we further increases the load then the value of BSFC start increase. And here it can be seen that the value of BSEC at higher load or even at moderate load is very close in case of different fuels.

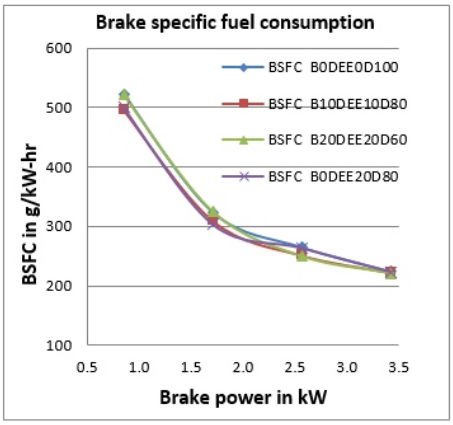

Fig. 2.Variation of BSFC with brake power

Brake specific energy consumption is the ratio of energy obtained by burning fuel for an hour to the actual energy or Brake power obtained at the wheels. It is indicative of how effectively the energy obtained from the fuel is reaching the wheels. In the following Fig. 3, throughout the brake power variation, change in BSEC value with different fuel blends is not that much.

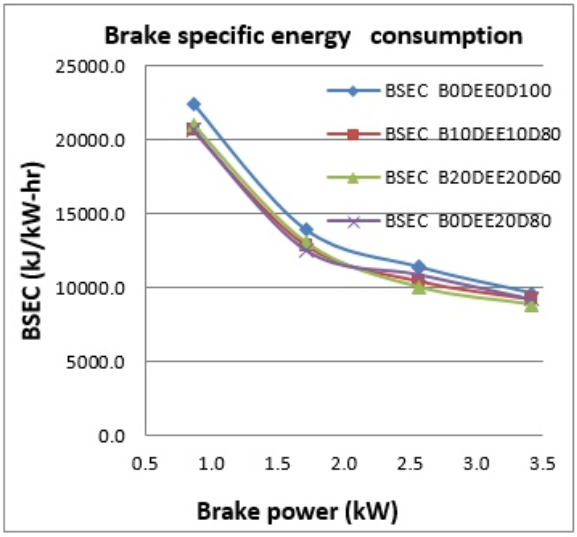

Fig. 3.Variation of BSEC with brake power

Even at full load, it is negligible with B20DEE20D60 having minimum BSEC, that shows fuel burnt per unit brake power is minimum for this blend.

Here Fig. 4 represents the variation of brake thermal efficiency with brake power for different fuels. As the load increases the BTE start rising. The value of BTE at any load show small variation from fuel to fuel.

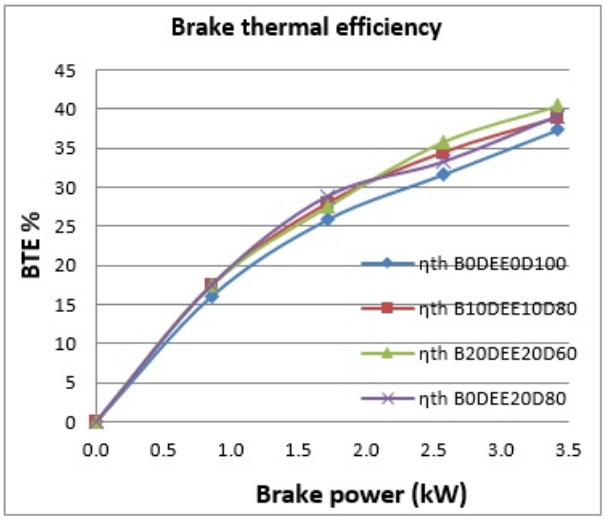

Fig. 4.Brake Thermal Efficiency variations

Exhaust gas temperature (EGT) shows the amount of heat taken away with the flue gases, hence showing fuel's inefficient utilization. Therefore its value should be minimum. In Fig. 5, it could be seen that at 50-100% load, B20DEE20D60 is having minimum or equal value of T6 (exhaust gas temperature) as compared to other fuel blends.

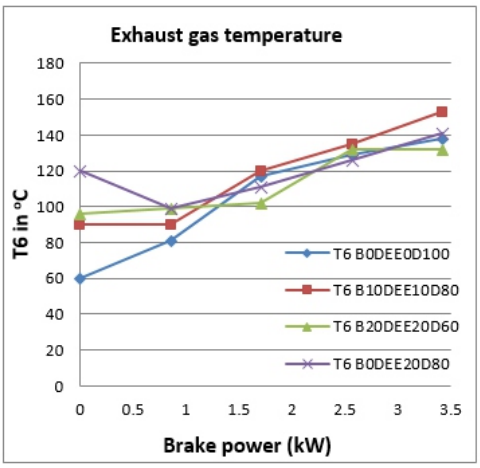

Fig. 5.Variation in EGT with brake power

Emission characteristics:

Fig. 6 shows the variation of CO with brake power for different percentage of blends. It is formed as a result of incomplete combustion. CO emissions are higher at lower loads. This due to fact that at low load condition, although DEE has higher cetane number, its latent heat of evaporation is slightly higher than that of diesel; as result there is not enough vaporization and hence very less time to burn fuel completely that results in considerable increase in CO emissions.

At higher loads, enough time available for combustion to occur, better mixing and inbuilt fuel oxygen that results in complete combustion and hence slightly reduces the CO emissions, for blends at high load. At full load, there is no significant change between the fuels for CO emissions. The blends of DEE and diesel have lower CO emissions at full load signifying the complete combustion whereas biodiesel addition to this blend relatively increase the CO emission at 75% of full load, though the difference is negligible throughout all load variations.

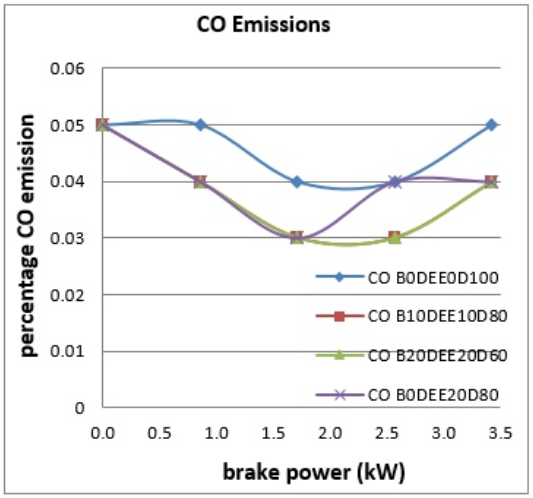

Fig. 6.Variation in CO with brake power

In Fig. 7 represent the emission of unburned hydrocarbons with respect to brake power. As we increases the load the amount of unburned hydrocarbon emission varies without showing any consistent nature. Addition of biodiesel to DEE-diesel blend is making the conditions better by providing better combustion and having minimum HC emissions at full load. The reduction of unburned hydrocarbon signifies the improvement in the combustion properties of fuel.

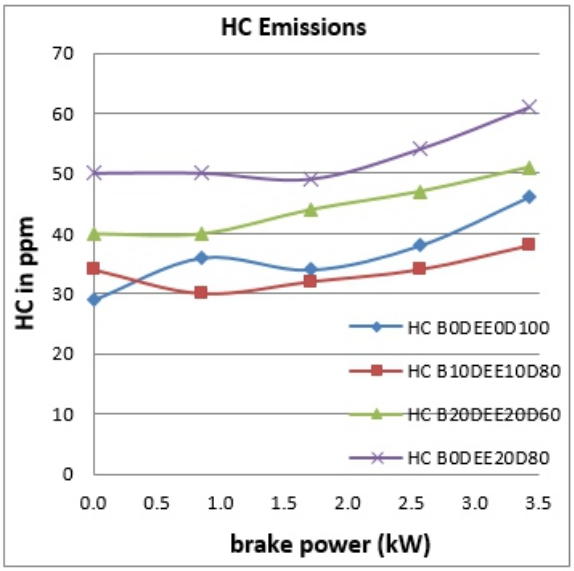

Fig. 7. HC emissions vs brake power

10% biodiesel with 10% DEE in diesel is proven to be the best fuel with regards to HC emissions. The HC are one of the major pollutants thus reduction of HC by addition of DEE-biodiesel is a very welcome outcome. It can be seen that the HC emissions for all the fuel blends are higher with the increase being higher in the percentage of diethyl ether in the blend. As known, the formation of unburned HC originates from various sources and varies widely with operating conditions. The increase of HC may be due to the higher latent heat of evaporation of diethyl ether causing lower combustion temperature, especially the temperature near the cylinder walls during the mixture formation. In this case more HC will be produced from the cylinder boundary.

Fig. 8 represents the trends of emission of NOx with respect to brake power. The NO emissions are very harmful and cause acid rain. As increased the load the NOx emission increased for all types of fuel.

The NOx emission reduced sharply when shifted from diesel to blended fuel. At no load condition the variation in NOx emission for diesel and B10DEE10D80 were almost same. And at peak load the variation is more for B0DEE20D80 fuel as well as B20DEE20D60 fuel.

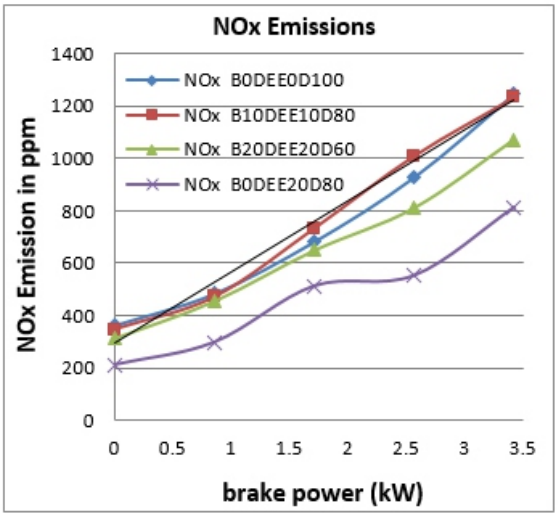

Fig. 8. NOx emissions variation with brake power

The Fig.9 represents the variation of emission of CO_2 with respect to brake power. The percentage of CO_2 in total emission increased when load is increased, this is mainly due to incomplete combustion. When DEE is blended with biodiesel and diesel there is increase in the percentage of the amount of CO_2 in exhaust gases at full load. Diesel is having minimum CO_2 emissions at full load. The increase of CO_2 is welcome because it signifies complete combustion. And hence blending with DEE is a good option to reduce the demand of diesel.

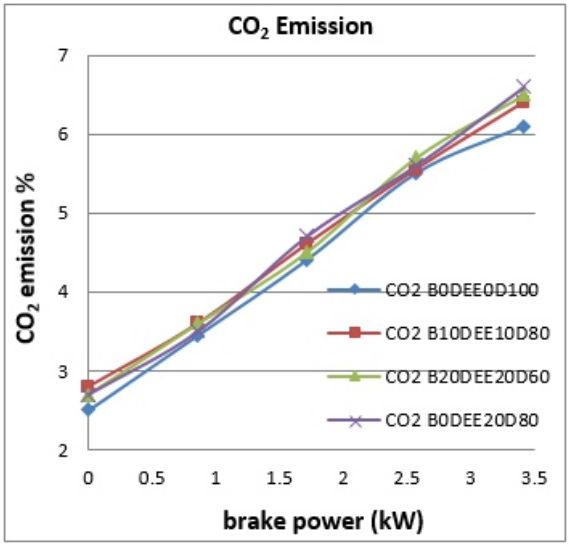

Fig. 9. Carbon dioxide (CO_2) variation with brake power

The smoke meter readout displays the smoke density giving a measure of the efficiency of combustion. The amount of smoke is shown in terms of Hart ridge Smoke Units (HSU). From the Fig. 10, we can easily conclude that smoke opacity i.e.

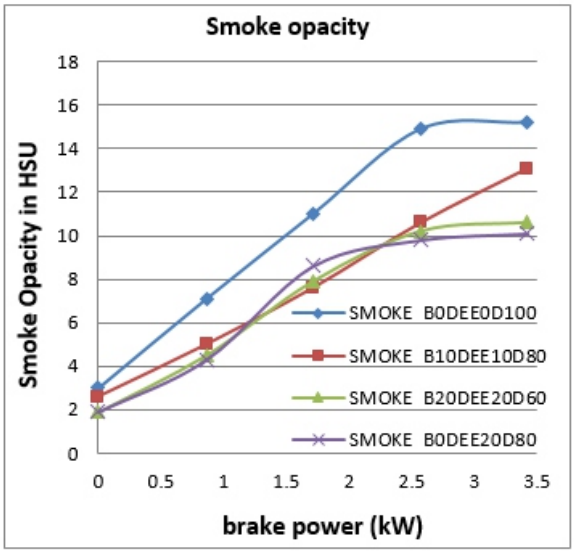

Fig. 10. Smoke opacity variation with brake power

considered as an indicator of dry soot emissions, as well as particulate matter emissions, which have soot as one of their main components, are both noticeably reduced with biodiesel blends. Value is higher in case of combustion with diesel as compared to others.

Since the smoke is mainly produced in the diffusive combustion phase, the addition of oxygenated fuel can overcome poor mixing of the fuel with air and leads to improvement in diffusive combustion .The reason for the fluctuations may explained by the fact that the properties of DEE such as its oxygen content and its latent heat of vaporization (LHV) are in competition. In the other words, its oxygen content leads to smoke reduction and its high LHV decreases the combustion temperature.

4. CONCLUSIONS

With thorough analysis of obtained result it can be concluded that the Biodiesel, diethyl ether and diesel blend is very beneficial to use as a feedstock for CI engine. The heating value of the blends decreases with addition of DEE.

- From the various DEE-Biodiesel blends tested, the B20DEE20D60 blend is found to be the optimum blend on the basis of emission and performance characteristics.
- DEE and biodiesel blended fuel does not affect mechanical efficiency, BSEC and brake thermal efficiency (BTE) negatively i.e. the above parameters are almost similar in case of all fuels.

- Use of DEE addition to diesel fuel and biodiesel increases the BTE in a general trend. BTE rises 8.32% with blend B20DEE20D60 with respect to neat diesel.
- There is increase in the CO_2 emission at peak load for B0DEE20D80 which indicates the complete combustion i.e. combustion quality is improved when diesel is blended with diethyl ether.
- Smoke opacity reduces with addition of DEE to the blends.
- NOx emission of rich DEE blends i.e. B0DEE20D60 and B20DEE20D60is decreased drastically. The effect of DEE on NOx reduction is more effective than the other emissions.
- HC emissions produced were more and CO were almost same by DEE blends than baseline fuel.
- Considering the advantages and obstacles of DEE, diesel fuel and biodiesel; and utilization of their combinations in suitable ratio can amplify their advantages and overcome their shortcomings.

REFERENCES

1.V. Edwin Geo, G. Nagarajan, B. Nagalingam, 2010, Studies on improving the performance of rubber seed oil fuel for diesel engine with DEE port injection, Fuel 89,pp. 3559–3567
http://www.sciencedirect.com/science/article/pii/S0016236110002619

2.S. Sivalakshmi, T. Balusamy, 2013, Effect of biodiesel and its blends with diethyl ether on the combustion, performance and emissions from a diesel engine, Fuel 106, pp. 106–110
http://www.sciencedirect.com/science/journal/00162361/106

3.Ismet Sezer, 2011, Thermodynamic, performance and emission investigation of a diesel engine running on dimethyl ether and diethyl ether, International Journal of Thermal Sciences 50, pp. 1594-1603
https://www.researchgate.net/publication/232410179_Thermodynamic_performance_and_emission_investigation_of_a_diesel_engine_running_on_dimethyl_ether_and_diethyl_ether

4.Brent, Bailey, Steve Guguen and Jimell Erwin, "Diethyl Ether (DEE)as a Renewable fuel", 972978, SAE

5.Anh N. Phan, Tan M. Phan, 2008, Biodiesel production from waste cooking oils, Fuel 87, pp. 3490–3496
https://www.researchgate.net/publication/222078826_Biodiesel_Production_from_Waste_Cooking_Oils

6.Banapurmath NR, Khandal SV, RanganathaSwamy and Chandrashekar TK, 2015,Alcohol (Ethanol and Diethyl Ethyl Ether)-Diesel Blended Fuels for Diesel Engine Applications-A Feasible Solution, Adv Automob Eng, 4(1), pp. 100-117
http://www.omicsgroup.org/journals/alcohol-ethanol-and-diethyl-ethyl-etherdiesel-blended-fuels-for-dieselengine-applicationsa-feasible-solution-2167-7670-1000117.php?aid=59635

7.A.M. Ashraful, H.H. Masjuki, M.A. Kalam, I.M. Rizwanul Fattah, S. Imtenan, S.A. Shahir, H.M. Mobarak, 2014, Production and comparison of fuel properties, engine performance, and emission characteristics of biodiesel from various non-edible vegetable oils: A review, Energy Conversion and Management 80, pp. 202–228 https://www.researchgate.net/publication/260194211_Production_and_comparison_of_fuel_properties_engine_performance_and_emission_characteristics_of_biodiesel_from_various_non-edible_vegetable_oils_A_review

8.Obed M. Ali, Rizalman Mamat and Che Ku M. Faizal , 2013, Effects of Diethyl Ether Additives on Palm Biodiesel Fuel Characteristics and Low Temperature Flow Properties, International Journal of Advanced Science and Technology, Vol. 52, pp. 111-120
http://www.sersc.org/journals/IJAST/vol52/10.pdf

9.Masoud Iranmanesh , J.P.Subrahmanyam , M.K.G.Babu, 2008, Application of Diethyl Ether to reduce smoke and NOx emissions simultaneously with Diesel and Biodiesel fuelled engines, ASME International Mechanical Engineering Congress and Exposition, IMECE-69255, pp. 1-8
http://science.fire.ustc.edu.cn/download/download1/paper/proceedings/ASME2008/data/pdfs/trk-3/IMECE2008-69255.pdf
10.Magín Lapuerta, José M. Herreros, Lisbeth L. Lyons, Reyes García-Contreras, Yolanda Briceño, 2008, Effect of the alcohol type used in the production of waste cooking oil biodiesel on diesel performance and emissions, Fuel 87, pp. 3161–3169https://www.researchgate.net/publication/222246723_Effect_of_the_alcohol_type_used_in_the_production_of_waste_cooking_oil_biodiesel_on_diesel_performance_and_emissions
11. Ni ZHANG, Zuohua HUANG, Xiangang WANG, Bin ZHENG, 2011,Combustion and emission characteristics of a turbo-charged common rail diesel engine fuelled with diesel-biodiesel-DEE blends, Front. Energy, 5(1): pp. 104–114
https://www.researchgate.net/publication/226897631_Combustion_and_emission_characteristics_of_a_turbo-charged_common_rail_diesel_engine_fuelled_with_diesel-biodiesel-DEE_blends
12. Y. Zhang, M.A. Dub, D.D. McLean, M. Kates, 2003,Biodiesel production from waste cooking oil: 1. Process design and technological assessment, Bio resource Technology, 89,pp. 1–16
http://www.ncbi.nlm.nih.gov/pubmed/12676496
13. S Sivalakshmi and T Balusamy, 2011,Effect of biodiesel and its blends with oxygenated additives on performance and emissions from a diesel engine, Journal of Scientific and industrial research, Vol. 70, pp. 879-883
http://nopr.niscair.res.in/handle/123456789/12685
14. K.R. Patil, S S. Thipse, 2015,Experimental investigation of CI engine combustion, performance and emissions in DEE–kerosene–diesel blends of high DEE concentration, Energy Conversion and Management 89,pp. 396–408
http://www.sciencedirect.com/science/article/pii/S0196890414009030
15. B. Sachuthananthan and K. Jeyachandran, 2007,combustion, performance and emission characteristics of water-biodiesel emulsion as fuel with DEE as ignition improver in a DI diesel engine, Journal of Environmental Research And Development Vol. 2(2), pp. 164-172 http://www.jerad.org/ppapers/dnload.php?vl=2&is=2&st=164

Instructions for Authors

Essentials for Publishing in this Journal

1 Submitted articles should not have been previously published or be currently under consideration for publication elsewhere.

2 Conference papers may only be submitted if the paper has been completely re-written (taken to mean more than 50%) and the author has cleared any necessary permission with the copyright owner if it has been previously copyrighted.

3 All our articles are refereed through a double-blind process.

4 All authors must declare they have read and agreed to the content of the submitted article and must sign a declaration correspond to the originality of the article.

Submission Process

All articles for this journal must be submitted using our online submissions system. http://enrichedpub.com/ . Please use the Submit Your Article link in the Author Service area.

Manuscript Guidelines

The instructions to authors about the article preparation for publication in the Manuscripts are submitted online, through the e-Ur (Electronic editing) system, developed by **Enriched Publications Pvt. Ltd**. The article should contain the abstract with keywords, introduction, body, conclusion, references and the summary in English language (without heading and subheading enumeration). The article length should not exceed 16 pages of A4 paper format.

Title

The title should be informative. It is in both Journal's and author's best interest to use terms suitable. For indexing and word search. If there are no such terms in the title, the author is strongly advised to add a subtitle. The title should be given in English as well. The titles precede the abstract and the summary in an appropriate language.

Letterhead Title

The letterhead title is given at a top of each page for easier identification of article copies in an Electronic form in particular. It contains the author's surname and first name initial .article title, journal title and collation (year, volume, and issue, first and last page). The journal and article titles can be given in a shortened form.

Author's Name

Full name(s) of author(s) should be used. It is advisable to give the middle initial. Names are given in their original form.

Contact Details

The postal address or the e-mail address of the author (usually of the first one if there are more Authors) is given in the footnote at the bottom of the first page.

Type of Articles

Classification of articles is a duty of the editorial staff and is of special importance. Referees and the members of the editorial staff, or section editors, can propose a category, but the editor-in-chief has the sole responsibility for their classification. Journal articles are classified as follows:

Scientific articles:

1. Original scientific paper (giving the previously unpublished results of the author's own research based on management methods).

2. Survey paper (giving an original, detailed and critical view of a research problem or an area to which the author has made a contribution visible through his self-citation);

3. Short or preliminary communication (original management paper of full format but of a smaller extent or of a preliminary character);

4. Scientific critique or forum (discussion on a particular scientific topic, based exclusively on management argumentation) and commentaries. Exceptionally, in particular areas, a scientific paper in the Journal can be in a form of a monograph or a critical edition of scientific data (historical, archival, lexicographic, bibliographic, data survey, etc.) which were unknown or hardly accessible for scientific research.

Professional articles:

1. Professional paper (contribution offering experience useful for improvement of professional practice but not necessarily based on scientific methods);
2. Informative contribution (editorial, commentary, etc.);
3. Review (of a book, software, case study, scientific event, etc.)

Language

The article should be in English. The grammar and style of the article should be of good quality. The systematized text should be without abbreviations (except standard ones). All measurements must be in SI units. The sequence of formulae is denoted in Arabic numerals in parentheses on the right-hand side.

Abstract and Summary

An abstract is a concise informative presentation of the article content for fast and accurate Evaluation of its relevance. It is both in the Editorial Office's and the author's best interest for an abstract to contain terms often used for indexing and article search. The abstract describes the purpose of the study and the methods, outlines the findings and state the conclusions. A 100- to 250- Word abstract should be placed between the title and the keywords with the body text to follow. Besides an abstract are advised to have a summary in English, at the end of the article, after the Reference list. The summary should be structured and long up to 1/10 of the article length (it is more extensive than the abstract).

Keywords

Keywords are terms or phrases showing adequately the article content for indexing and search purposes. They should be allocated heaving in mind widely accepted international sources (index, dictionary or thesaurus), such as the Web of Science keyword list for science in general. The higher their usage frequency is the better. Up to 10 keywords immediately follow the abstract and the summary, in respective languages.

Acknowledgements

The name and the number of the project or programmed within which the article was realized is given in a separate note at the bottom of the first page together with the name of the institution which financially supported the project or programmed.

Tables and Illustrations

All the captions should be in the original language as well as in English, together with the texts in illustrations if possible. Tables are typed in the same style as the text and are denoted by numerals at the top. Photographs and drawings, placed appropriately in the text, should be clear, precise and suitable for reproduction. Drawings should be created in Word or Corel.

Citation in the Text

Citation in the text must be uniform. When citing references in the text, use the reference number set in square brackets from the Reference list at the end of the article.

Footnotes

Footnotes are given at the bottom of the page with the text they refer to. They can contain less relevant details, additional explanations or used sources (e.g. scientific material, manuals). They cannot replace the cited literature.
The article should be accompanied with a cover letter with the information about the author(s): surname, middle initial, first name, and citizen personal number, rank, title, e-mail address, and affiliation address, home address including municipality, phone number in the office and at home (or a mobile phone number). The cover letter should state the type of the article and tell which illustrations are original and which are not.

Address of the Editorial Office:

Enriched Publications Pvt. Ltd.
S-9,IInd FLOOR, MLU POCKET,
MANISH ABHINAV PLAZA-II, ABOVE FEDERAL BANK,
PLOT NO-5, SECTOR -5, DWARKA, NEW DELHI, INDIA-110075,
PHONE: - + (91)-(11)-45525005